Delongia gen. nov., a new genus of Polytrichaceae (Bryophyta) with two disjunct species in East Africa and the Himalaya

Neil E. Bell,[1,2,3] Isuru U. Kariyawasam,[4] Terry A.J. Hedderson[5] & Jaakko Hyvönen[3]

1 *Royal Botanic Garden Edinburgh, 20a Inverleith Row, Edinburgh EH3 5LR, Scotland, U.K.*

2 *Botanical Museum, Finnish Museum of Natural History, University of Helsinki, P.O. Box 7, 00014 Helsinki, Finland*

3 *Department of Biosciences (Biocenter 3),University of Helsinki, P.O. Box 65, 00014 Helsinki, Finland*

4 *Department of Botany, University of Sri Jayewardenepura, Gangodalwila, Nugegoda, Sri Lanka*

5 *Department of Biological Sciences and Bolus Herbarium, University of Cape Town, Private Bag, 7700 Rondebosch, South Africa*

Author for correspondence: *Neil E. Bell, N.Bell@rbge.ac.uk*

ORCID: NEB, http://orcid.org/0000-0002-2401-2968; IUK, http://orcid.org/0000-0002-2527-3502; TAJH, http://orcid.org/0000-0002-3537-6599

Abstract Although the family Polytrichaceae contains the largest and structurally most complex of all mosses, a number of distantly related lineages share a relatively reduced gametophytic morphology and have historically been conflated under polyphyletic genera, most notably *Oligotrichum* s.l. Based on new and newly identified collections, phylogenetic analysis of nucleotide data, scanning electron microscopy and relaxed-clock divergence time estimation, we recognise *O. glaciale* and *O. cavallii* under the new genus *Delongia*, which is more closely related to *Psilopilum*, *Atrichum* and *Steereobryon* than to *Oligotrichum*. The two species are mutually highly distinct in both morphological and molecular characters, with *D. glacialis* occurring across the Himalaya from Pakistan to Yunnan and *D. cavallii* found in the East African Rift Mountains and on the island of Réunion. Divergence time estimation suggests that the lineages represented by the extant species diverged from each other around the Oligocene-Miocene boundary (~23 Ma), contemporaneous with the origins of the East African Rift system and ongoing uplift of the Qinghai-Tibetan Plateau, while *Delongia* most likely shares a common ancestor in the Eocene (56–34 Ma) either with the arctic-subarctic genus *Psilopilum* or with *Atrichum* and *Steereobryon*.

Keywords bryophyte phylogeny; East African Rift; mosses; *Oligotrichum*; relaxed-clock dating; Réunion

Supplementary Material The Electronic Supplement (Figs. S1–S2; Appendix S1 with full species descriptions) is available in the Supplementary Data section of the online version of this article at http://www.ingentaconnect.com/content/iapt/tax. The original matrix was submitted to TreeBase (http://purl.org/phylo/treebase/phylows/study/TB2:S17555).

■ INTRODUCTION

The Polytrichaceae (Polytrichales) are a phylogenetically and morphologically distinct lineage of mosses with a world-wide distribution. Most members have a characteristic leaf morphology, with photosynthetic lamellae on the adaxial surface, and a unique spore dispersal mechanism based on a nematodontous peristome and a membranous epiphragm. The most prominent dimension of gametophyte diversity is a continuum between robust plants with extensive lamellae, differentiated lamellar end-cells, broad nerves and sharply demarcated sheathing leaf bases on the one hand, and smaller plants with reduced lamellae, undifferentiated lamellar end-cells, narrow nerves and less differentiated sheathing leaf bases on the other (Smith, 1971; Bell & Hyvönen, 2012). While robust and gametophytically complex morphologies appear to have arisen early within the evolution of the family (e.g., *Dawsonia* R.Br.; Hyvönen & al., 1998; Bell & Hyvönen, 2010a), a number of genera are characterised by gametophytic reduction as described above (e.g., *Itatiella* G.L.Sm., *Oligotrichum* DC., *Psilopilum* Brid., while others have some reduced features and/or contain some species that are reduced (e.g., *Atrichum* P.Beauv., *Pogonatum* P.Beauv.). Many of these species are adapted to exposed and relatively extreme habitats, either at high altitude or in cold oceanic environments (Bell & Hyvönen, 2012). Given the malleability of the gametophyte, sporophyte characters appear to define genera most discretely within the family, especially for groups having simplified gametophyte morphologies (Bell & Hyvönen, 2010a, 2012).

Recent research, using molecular phylogenetic characters (Bell & Hyvönen, 2010a, 2012), has confirmed earlier suggestions (Smith, 1971) that nearly all of the species with distinctly southern hemisphere distributions traditionally placed in *Oligotrichum* are more closely related to other austral taxa than to the predominantly northern hemisphere *Oligotrichum* species. This is additionally supported by sporophyte morphology and many of these species have been newly placed in *Itatiella* (Bell & Hyvönen, 2012). Conversely, nearly all of the northern species form a well-supported group with imprecisely resolved

affinities to a *Psilopilum/Atrichum/Steereobryon* clade and to species of *Polytrichastrum* G.L.Sm. (Bell & Hyvönen, 2010a, 2012). An additional observation in Bell & Hyvönen (2012) was that the East African montane species *O. cavallii* (Negri) G.L.Sm. and a specimen resembling *O. glaciale* C.C.Towns. collected at 4200 m in Pakistan by the third author appear to be closely related to each other, while falling outside of the clade of northern hemisphere *Oligotrichum* species and apparently having a closer relationship to *Psilopilum*, *Atrichum* and *Steereobryon*. This study aims to investigate the relationships, morphology and distribution of this lineage, place it on a secure phylogenetic and taxonomic footing and explore scenarios for the timing of its differentiation as well as the ancestral states of key characters.

The basionym of *Oligotrichum cavallii*, *Catharinea cavallii* Negri, was described in 1908 from sterile material collected at 3800 m in the Ruwenzori Mountains (part of the Western Rift Mountains) in present-day Uganda. The sporophyte was unknown until collections from Mt. Mikeno (Virunga Mountains, Democratic Republic of the Congo) revealed obovoid capsules with "swollen cells" in the apophysis (the differentiated sterile region at the base of the capsule), on the basis of which Potier de la Varde and Thériot (Potier de la Varde, 1943) described the new genus "*Spoggodera*" in French. However, this name was never validly published with a Latin description. Smith (1971) placed the species in *Oligotrichum* on the basis of examination of sterile material and the existing description of the sporophyte. The range of the species has since been extended to Rwanda (Mt. Sabinyo, Virunga Mountains) and to the Eastern Rift Mountains in Tanzania (Mt. Kilimanjaro, between 2000 m and 3000 m) and Kenya (Mt. Kenya, from 3200 m to 3400 m). Additionally it was collected on Mt. Elgon during the British Bryological Society (BBS) expedition to Uganda in 1998. Finally, in 2011 the third author made collections at 2300 m on the island of Réunion, extending its known range beyond mainland East Africa (Ellis & al., 2014).

Oligotrichum glaciale was described in 1998 from two sterile collections made at 3800 m in Kashmir, India, in 1989 (Townsend, 1998). Another sterile specimen, collected by the third author in Pakistan in 1998, was initially assigned to this species, although it was treated as unnamed by Bell & Hyvönen (2012) as it seemed to differ slightly from the description of *O. glaciale*, and material of the latter was not available for comparison at the time. Although differing from each other, the gametophyte morphologies of *O. cavallii* and *O. glaciale* are both somewhat atypical for the genus (see Discussion).

In 2013 the second author completed a taxonomic study of *Oligotrichum* in the Sino-Himalayan region as part of his M.Sc. studies at the Royal Botanic Garden, Edinburgh (E). As part of this work the collections made by David Long in the Himalaya and Sino-Himalaya were examined, and eight further specimens corresponding to *O. glaciale* were identified from Sikkim, Nepal and Yunnan, including a single specimen from Sikkim with sporophytes. This material, together with the new specimens of *O. cavallii* from Réunion, provide the basis for an expanded molecular phylogenetic study to test the findings of Bell & Hyvönen (2012), as well as the monophyly of each

species as represented by geographically disjunct exemplars. Furthermore, the identification of sporophytes of *O. glaciale* for the first time allows comparison with those of *O. cavallii*. The "spongy" tissue of the apophysis in *O. cavallii* (the inspiration for the invalidly published name "*Spoggodera*") is investigated further by examination of sporophytes of both species using scanning electron microscopy (SEM). We additionally use uncorrelated relaxed-clock dating methods in an attempt to place some bounds on the temporal origins of the clade. Finally, the ancestral states of some key characters shared between these species, *Oligotrichum* and *Psilopilum* are reconstructed.

Here we describe *Delongia* gen. nov. based on these studies. The sporophyte of *Oligotrichum glaciale* is newly described and aspects of ecology and biogeography briefly discussed.

■ MATERIALS AND METHODS

Sampling. — The study of Bell & Hyvönen (2012), which investigated relationships within and between groups of species traditionally recognised in *Oligotrichum* using sequences from five genomic regions (the nuclear 18S gene, the mitochondrial *nad5* gene, the 3′ half of the chloroplast *rbcL* gene, the chloroplast *rps4* gene and downstream intergenic spacer, and the chloroplast *trnL-trnF* region), included a single specimen ("Pakistan specimen") now identified unambiguously as *O. glaciale*, as well as a specimen of *O. cavallii* from Mt. Elgon in Uganda. Additionally, DNA sequences from two of these five regions (*rps4*, *trnL*) were obtained from a second collection of *O. cavallii* from Mt. Kilimanjaro in Tanzania, although these were not used in the final analyses because they were identical to the corresponding sequences from the Ugandan specimen and the missing data would have artificially reduced support values. For this study we included two further specimens of *O. cavallii* from Réunion as well as two more specimens of *O. glaciale*, from Sikkim in India and Yunnan in China. All five of the above genomic regions were sequenced for all of the new specimens except that the *rbcL* region could not be obtained for the specimen of *O. glaciale* from Sikkim. Sampling of both species thus included specimens completely or nearly completely spanning their known ranges (Fig. 1); from Uganda to Réunion in the case of *O. cavallii*, and across the Himalaya from Pakistan to Yunnan for *O. glaciale*. In the case of *O. glaciale*, the collections are approximately equidistant, encompassing in the western Himalaya in Northern Pakistan, the Prek Chhu valley in Sikkim (central greater Himalaya) and the Sino-Himalaya in Yunnan. For *O. cavallii*, sampling includes the easternmost outpost of the known range on Réunion as well as Mt. Elgon to the west of the Eastern Rift Valley in mainland Africa, while the limited data from the Mt. Kilimanjaro specimen (above; Bell & Hyvönen, 2012) nominally extends sampling to the east of the Eastern Rift Valley.

We constructed a matrix including extensive outgroup sampling from the Polytrichales by selecting appropriate taxa from datasets used in some of our previous studies (Bell & Hyvönen, 2010a, b, 2012). All genomic regions were sampled at least partially for all terminals except as detailed above

for samples of *O. cavallii* and *O. glaciale*, and excepting the *trnL-F* region for *Alophosia azorica* (Renauld & Cardot) Cardot. Total missing data in the aligned matrix was 4.1%. Sampling (Appendix 1) focused on the large "northern hemisphere clade" of Polytrichales (*Atrichum, Oligotrichum* s.str., *Pogonatum, Polytrichastrum, Polytrichum* Hedw., *Psilopilum, Steereobryon*; Bell & Hyvönen, 2010a), with reduced but representative sampling from the predominantly southern hemisphere genera (*Dawsonia, Dendroligotrichum* (Müll.Hal.) Broth., *Hebantia, Itatiella, Notoligotrichum, Polytrichadelphus* (Müll.Hal.) Mitt.) and from the earliest-diverging plesiomorphically non-peristomate genera (*Alophosia* Cardot, *Lyellia* R.Br., *Bartramiopsis* Kindb.). Denser sampling was necessary within the northern hemisphere clade due to ambiguous resolution between some groups that are individually clearly monophyletic (Bell & Hyvönen, 2010a, 2012), these being the *Polytrichum*/*Pogonatum* clade, the *Atrichum*/*Steereobryon* clade, *Oligotrichum* s.str., *Psilopilum*, the core *Polytrichastrum* clade, *Polytrichastrum sexangulare* and *Polytrichastrum sphaerothecium* (Besch.) J.-P.Frahm. To make analyses more tractable we did not include all species for which we have data within these securely monophyletic groups.

Laboratory methods. — Genomic DNA was isolated using the Invisorb spin plant mini kit (Invitek, Berlin, Germany) and eluted DNA stored in the supplied buffer. PCR amplifications were performed in 50 µl reactions with 1.25 U Fermentas DreamTaq polymerase and DreamTaq buffer (Fermentas, Burlington, Ontario, Canada), 200 µM dNTPs and 0.3 µM of each primer. Protocols for PCR and primer sequences were as detailed in Bell & Hyvönen (2010a). Purification and sequencing of PCR products was carried out by Macrogen Europe (Amsterdam, The Netherlands) with the same sequencing primers as in Bell & Hyvönen (2010a).
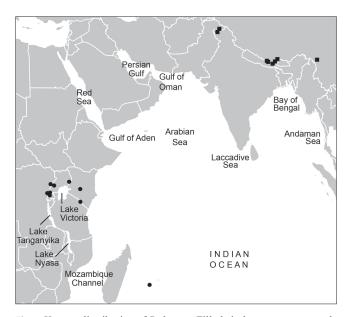

Fig. 1. Known distribution of *Delongia*. Filled circles represent records of *D. cavallii*, filled squares *D. glacialis*. Note the occurrence of *D. cavallii* on the island of Réunion as well as across the East African Rift Mountains.

Phylogenetic analysis. — Sequences were manually aligned using PhyDE v.0.997 (Müller & al., 2011) according to the principles outlined in Kelchner (2000). For the protein coding regions (*rbcL*, the *rps4* gene, *nad5* exon) there was no alignment ambiguity, while for 18S ambiguity was effectively restricted to a single 10-bp region that was excluded prior to analysis. For the non-coding regions (*nad5* intron, most of *trnL-F*, *rps4-trnS* intergenic spacer) the majority of the alignment was unambiguous, with ambiguity mostly restricted to short mono- and dinucleotide repeats (generally of A and T), which were excluded. Also excluded was a previously identified hairpin-associated inversion in the *trnL-F* region that is variably present and known to be highly homoplastic (Quandt & al., 2004, 2007; Quandt & Stech, 2005; Bell & al., 2007). Our original matrix (TreeBase: http://purl.org/phylo/treebase/phylows/study/TB2:S17555) comprised 73 terminals and 5753 characters. Two of the concatenated sequences from exemplars of *Oligotrichum cavallii* were identical at all alignment positions (including missing data) and the duplicate terminal was removed from some analyses. Phylogenetic analyses were conducted using parsimony, maximum likelihood (ML) and Bayesian approaches, with gaps treated as missing data. These methods involve different theoretical assumptions (while also having many other assumptions in common), and any conflicts between the results may assist in assessing the validity of these as they relate specifically to the data in question. Lack of conflict in turn implies that the phylogenetic signal is robust against these different assumptions.

For the model-based approaches seven partitions were defined, with separate partitions for each homogenous genomic region and for sizeable discrete coding or non-coding units within mixed regions. The *trnL-F* region was treated as a single partition due to the short lengths of its three discrete elements (the *trnL* gene, the group I intron and the *trnL-F* intergenic spacer). Thus partitions were defined for 18S, *rbcL*, the *rps4* gene, the *rps4-trnS* intergenic spacer, the concatenated coding region of the *nad5* gene, the *nad5* group I intron, and the *trnL-F* region in its entirety. MrModeltest v.2.2 (Nylander, 2004) was used for initial estimation of the best-fitting models for each partition using the Akaike information criterion (Akaike, 1974). For ML analysis the most complex model selected for any one partition was applied independently to all partitions, while for Bayesian analysis separate analyses were performed using the most complex model independently for all partitions (as under ML) and using different models independently for partitions where these were selected as optimal by MrModeltest, in order to assess the impact of heterogenous vs. homogenous models. In our divergence time analyses using BEAST (see below) we additionally assessed the statistical significance of heterogenous vs. homogenous models using Bayes factors. Finally, under all three methods analyses were conducted separately for the total combined dataset and for the combined chloroplast and mitochondrial dataset (i.e., excluding 18S). Previous results have indicated that the 18S region is incongruent with other regions for localised relationships within the Polytrichales, most notably the monophyly or otherwise of *Pogonatum*, and that this may be due to ancient hybridisation events in specific

clades (Bell & Hyvönen, 2010a). Although there was no evidence of incongruence between these markers for the genera we are addressing here, we preferred to compare topologies with and without 18S, which as a highly conserved gene might also be incongruent with other regions due to homoplasy induced by strong functional constraints (Bell & Hyvönen, 2010a).

ML analyses were conducted using RAxML v.7.4.2. (Stamatakis, 2006) with the raxmlGUI v.1.3 front end (Silvestro & Michalak, 2012). The "ML+thorough bootstrap" option within the raxmlGUI (RAxML option "-b" followed by an ML search) was used on the partitioned dataset, with 10 runs and 500 replications. Bayesian phylogenetic analyses were conducted using MrBayes v.3.1.2 x64 (Ronquist & Huelsenbeck, 2003). Partitions were unlinked to allow parameters other than topology to vary independently. In each analysis, three independent runs using the default prior settings, each with five chains ("temp" parameter = 0.15), were run simultaneously for 1×10^7 generations with trees sampled every 1000 generations. Adequate sampling from the cold chain at stationarity and convergence of independent runs was assessed by checking that the average standard deviation of split frequencies was <0.01, potential scale reduction factor (PSRF) values were near 1.00, effective sample sizes for each parameter were meaningful, and sampling from the posterior probability (PP) distribution was accurate as assessed by examination of log-likelihood trace files in Tracer v.1.6.0. The first 50% of trees (including those from the burn-in phase) were discarded and a majority-rule consensus tree constructed using the remaining sample.

Parsimony analyses were undertaken using several different programs and approaches. PAUP* analyses (PAUP* v.4.0b10, Swofford, 2002) were performed with stepwise random taxon addition and TBR branch swapping. Branches were collapsed when the maximum length was zero and all character transitions were equally weighted. Initial searches of 10,000 replications were performed saving only one tree on each replication (nchuck = 1, chuckscore = 1), followed by final searches with no limits on the number of trees saved (nchuck = 0), starting with the trees held in memory from the first step. Non-parametric bootstrap (BS) analyses were conducted on each dataset with 1000 replications of two full heuristic searches (settings as above) and maxtrees fixed at 3000. Additional parsimony analyses were performed with Nona v.2.0 (Goloboff, 1994) within the WinClada shell(Nixon, 2002), and TNT v.1.1 (Goloboff & al., 2003, 2008). Prior to these analyses we used the WinClada command "Mop uninformative characters". Unlike in the PAUP* analyses, branches were collapsed if their minimum length was zero (i.e., if an ancestor and descendant had the same state under any of the optimisations on the node). Nona analyses were performed using processor time as a seed to randomize the order of the terminals with the following settings: hold 30000 (holding a defined number of trees), 100 replications (search performed with multiple tree bisection–reconnection algorithm mult*max*), and hold/20 (to define the starting trees for each replication). TNT was then used to perform constrained searches to reveal how much longer the equally parsimonious trees (EPTs) would be if (1) *Oligotrichum cavallii* and *O. glaciale* were forced not to form a clade, and

(2) all species of *Oligotrichum* s.str. (Bell & Hyvönen, 2012) together with *O. cavallii* and *O. glaciale* were forced to form a clade (negative and positive constraints, respectively). These analyses were performed with the settings used for the Nona analyses as above (except that for the random seed, the default of one, plus four random numbers between 1 and 100 was used).

Divergence time estimation. — We used relaxed-clock methods as implemented within the program BEAST v.2.2.1 (Drummond & al., 2006; Drummond & Rambaut, 2007; Bouckaert & al., 2014) with uncorrelated lognormal rate variation between branches to estimate divergence times for selected clades. This was performed on the dataset excluding 18S to avoid increased analytical complexity due to topological conflict between 18S and the mitochondrial and chloroplast data for some groups unrelated to the target taxa (Bell & Hyvönen, 2010a and above). We initially used the path sampler GUI within the BEAST package to compare Yule and birth-death process tree models (Yule, 1925; Gernhard, 2008) as well as heterogenous and homogenous substitution models, with estimated marginal likelihood values from path sampling (Ogata, 1989; Gelman & Meng, 1998) used to calculate Bayes factors according to the significance table in Kass & Raftery (1995: 777). Path sampling, while computationally intensive, has recently been shown to substantially outperform previously widely used marginal likelihood estimators such as the harmonic mean estimator (Baele & al., 2012). Fifty path sampling steps were used with a chain length of 1×10^7, alpha value of 0.3 and a 50% burn-in, this being necessary to achieve adequate effective sample sizes. Results of these analyses were used to select the optimal combination of substitution and tree process models for subsequent analyses.

For final analyses runs were performed with MCMC chain lengths of 5×10^8, sampling parameters every 1×10^4 iterations. Log files were viewed in Tracer v.1.6.0 (Rambaut & al., 2014) to assess stationarity and effective sampling from the posterior distribution. Appropriate burn-in values were then selected prior to extracting values for geometric means of divergence times and 95% confidence intervals.

Unfortunately options for calibration within the Polytrichaceae are limited as only a small number of fossils are known. Fossils in Baltic amber attributed to *Atrichum* (Frahm, 2004) do provide one very useful reference point for a clade closely related to the target taxa. These plants have a number of features, including differentiated leaf borders and *Atrichum*-like lamellae, indicating clear affinities to either *Atrichum* or its monotypic sister lineage *Steereobryon*. Based on a youngest age for Baltic amber (Ritzkowski, 1999) of 37 million years we used these fossils as a minimum age constraint for the origin of the *Steereobryon+Atrichum* lineage taking into account phylogenetic uncertainty, i.e., the most recent common ancestor (MRCA) of the *Psilopilum*/*Steereobryon*/*Atrichum*/*Oligotrichum cavallii*/*O. glaciale* clade, by placing a uniform prior with a lower bound of 37.0 on this node.

Based on Newton & al. (2007) we also applied a constraint on the age of the MRCA of the Polytrichales in the form of a normally distributed prior with a mean of 230.53 Ma and a standard deviation of 22. This produces 95% quantiles in the

range 194.3–266.7, in line with the 90% lower and upper confidence intervals in Newton & al. (2007) of 206.73 and 253.04 respectively. We also applied relatively flexible priors on the substitution rates for each compartment based on published overall substitution rates for the chloroplast and mitochondrial genomes. We used normal distributions with means of 5×10^{-4} substitutions/site/million years and standard deviations of 1.5×10^{-4} for the ucld mean priors for the chloroplast compartments based on Palmer (1991) and Sanderson (2002), both of whom found overall plastid substitution rates around this value. For the two mitochondrial compartments we used normal distributions, with means of 1.09×10^{-4} and standard deviations of 5×10^{-5} based on the estimate of Gaut (1998) for overall embryophyte mitochondrial genome substitution rates.

Finally, in a separate experimental analysis we applied a calibration based on the phylogenetic position of the enigmatic fossil *Eopolytrichum antiquum* Konopka & al. (Konopka & al., 1997). The sporophyte of this plant, of early Campanian (late Cretaceous) age, has several features suggesting affinities to extant *Polytrichum* sect. *Polytrichum* and sect. *Juniperifolia* Brid. (but not *P.* sect. *Aporotheca* (Limpr.) N.E.Bell & Hyvönen), such as a mamillose, pitted exothecium (capsule epidermis), a "discoid" apophysis and echinulate spores. Other features, however, including terete capsule shape, absence of peristome teeth and retention of the epiphragm in the operculum are unknown in extant *Polytrichum* spp. and hint at a more distant relationship. Hyvönen & al. (2004) consistently found *Eopolytrichum* Konopka & al. in a clade with *Polytrichum* sect. *Polytrichum* and sect. *Juniperifolia* based on parsimony analysis including morphological characters, although with a jackknife support value of only 67%. We thus applied a minimum age constraint (using a uniform prior as above) of 80 Ma for the node representing the stem lineage of *Polytrichum* sect. *Polytrichum*+*P.* sect. *Juniperifolia*, i.e., the MRCA of the *Polytrichum* clade (including *P.* sect. *Aporotheca*), in this analysis. Due to uncertainty surrounding the underlying basis of this calibration we conducted further path sampling analyses (with settings as above) to statistically compare with Bayes factors the results of divergence time estimates obtained with and without the *Eopolytrichum* fossil calibration.

In both analyses we estimated divergence times for the *O. cavallii*/*O. glaciale* clade and the *Psilopilum*/*Steereobryon*/*Atrichum*/*Oligotrichum cavallii*/*O. glaciale* clade (monophyly enforced), as well as for a hypothetical *O. cavallii*/*O. glaciale*/*Psilopilum* clade (monophyly not enforced).

Ancestral character state reconstruction. — We examined probabilities for states of certain taxonomically critical morphological characters for the MRCAs of some key species groups. In particular, given that reduced adaxial lamellae have played a dominant role in historical concepts of *Oligotrichum* s.l., we were interested in whether the MRCA of *Oligotrichum* s.str. and any *Psilopilum*/*Steereobryon*/*Atrichum*/*Oligotrichum cavallii*/*O. glaciale* clade (all members of which also have reduced lamellae) was likely to have shared this feature, i.e., whether the character is homologous between these two groups of taxa. We also wished to explore whether the markedly concave leaf morphology shared between *Psilopilum* and *O. glaciale*

is likely to be homologous or independently derived, and to this end reconstruct states of this character for the MRCAs of the *O. cavallii*/*O. glaciale* clade, the *Psilopilum*/*O. cavallii*/*O. glaciale* clade and the *Psilopilum*/*Steereobryon*/*Atrichum*/*O. cavallii*/*O. glaciale* clade. We used the "MultiState" option within the program BayesTraits v.1.0 (Pagel & al., 2004; available at http://www.evolution.rdg.ac.uk) to reconstruct ancestral character states. A set of 5000 trees from the post-burn-in phase of one of the two MrBayes runs from analysis of the dataset excluding 18S was used as an input for all reconstructions. Both characters were treated as binary (adaxial lamellae reduced/not reduced, leaves concave/not concave). Lamellae were scored as reduced if they were more or less restricted to the costa, while this character was scored as unknown for *Alophosia azorica*, the earliest diverging lineage in the Polytrichales which primitively lacks lamellae (well-developed lamellae are present in *Lyellia* and *Dawsonia* and are assumed to have characterised the MRCA of all extant Polytrichales excluding *Alophosia*; see, e.g., Bell & Hyvönen, 2012). To obtain posterior distributions of models of evolution for each character, we used the reversible jump MCMC option within BayesTraits MultiState (Pagel & Meade, 2006). An exponential prior was seeded from a uniform hyperprior on the interval 0 to 30 (Pagel & al., 2004). The "addmrca" command was used to generate posterior distributions of likelihoods for ancestral character states for MRCAs of selected groups of taxa. This allows posterior distributions of MRCA states to be calculated even where MRCA nodes for a group are different between different sets of trees due to phylogenetic uncertainty. Analyses were conducted using 5×10^7 iterations, a burn-in of 1×10^7 and a sample frequency of 3000. The "ratedev" parameter was set to 3 for both characters, this value producing optimal ranges for acceptance rates (20%–30%).

Scanning electron microscopy. — Two whole capsules from one collection of *Oligotrichum glaciale* and two each from two collections of *O. cavallii* were selected for SEM, along with single exemplars of selected other taxa for comparison (*Psilopilum cavifolium* (Wilson) I.Hagen, *O. parallelum*, *O. austroaligerum* G.L.Sm., *O. aligerum* Mitt. and *O. obtusatum* Broth.). Vouchers are listed in Appendix 2. Only one collection of *O. glaciale* with sporophytes is known, with the capsules being slightly less than fully mature (the sporangia are mostly brown but none have dehisced naturally and the opercula do not detach easily).

Some specimens were fixed and subjected to critical point drying (CPD) before platinum coating, while others were platinum or gold palladium coated directly from untreated dry material. The former were fixed in 2% glutaraldehyde in 0.05 mol/l $NaPO_4$ buffer overnight at 20°C, postfixed in 1% OsO_4 in 0.05 mol/l $NaPO_4$ buffer for 2 h and then rinsed three times in dH_2O for 30 min (protocol adapted from Merced & Renzaglia, 2013). Dehydration in a graded ethanol series was followed by three final rinses in 100% ethanol prior to CPD in a Bal-Tec CPD 030 unit (Bal-Tec, Balzers, Liechtenstein). Most specimens were sputter-coated with platinum, mounted longitudinally on aluminium stubs and then examined using an FEI Quanta 250 Field Emission Gun SEM at the Electron Microscopy Unit of the Institute of Biotechnology, University

of Helsinki. Two specimens were sputter-coated with gold pal-ladium, mounted as above and examined using a Supra 55VP LEO SEM at the Electron Microscopy Suite of the Royal Botanic Garden, Edinburgh.

■ RESULTS

Molecular data and phylogeny estimation. — After exclusion of areas of significant alignment ambiguity in non-coding regions and of terminal areas containing large amounts of missing data, the alignment comprised a matrix of 5641 nucleotide characters, distributed between the different regions as listed in Table 1. Of these, 490 were parsimony informative (431 excluding 18S). The optimal models for each compartment selected using the Akaike criterion within MrModeltest are listed in Table 1, these favouring a heterogenous overall substitution model (as opposed to a uniform model with GTR+Γ+I applied to all compartments). This was corroborated by Bayes factors obtained from the path sampling analyses in BEAST, which favoured a heterogenous model employing a birth-death tree process (Table 2). Topologies obtained in the MrBayes analyses did not vary with model selection and nearly all PP values varied by less than 5%. Thus for Bayesian analysis only the results from compartmentalised heterogenous models will be presented.

Parsimony analysis under PAUP* resulted in 17,136 EPTs of length 1610 with a CI (consistency index) of 0.57 (Kluge & Farris, 1969) and RI (retention index) of 0.79 (Farris, 1989) for the dataset including 18S, and 42,624 EPTs of length 1416 (CI = 0.58, RI = 0.78) for the dataset excluding 18S. The Nona heuristic search produced 504 EPTs for the dataset with 18S and 1312 for the dataset without 18S, also of lengths 1610 and 1416 steps respectively. Consistent with Farris & al. (1996), this resulted in identical consensus trees to those obtained under PAUP* despite the much smaller number of EPTs. Constrained analyses with TNT on the datasets both with and without 18S showed that trees without an *Oligotrichum cavallii* and *O. glaciale* clade were six steps longer than those including this clade, and trees where all species currently placed in *Oligotrichum* were forced to form a clade were three steps longer than those obtained without this constraint.

All MrBayes analyses reached stationarity after 1×10^7 generations as determined by the criteria described above, although for the analyses excluding 18S, examination of trace files showed that some runs had a tendency to remain "stuck" in a slightly suboptimal sampling space. We thus ensured that samples chosen for posterior probability estimation were from runs that had reached the optimal sampling space, and that where abrupt transitions had occurred during analysis these were prior to the 50% burn-in cut-off point.
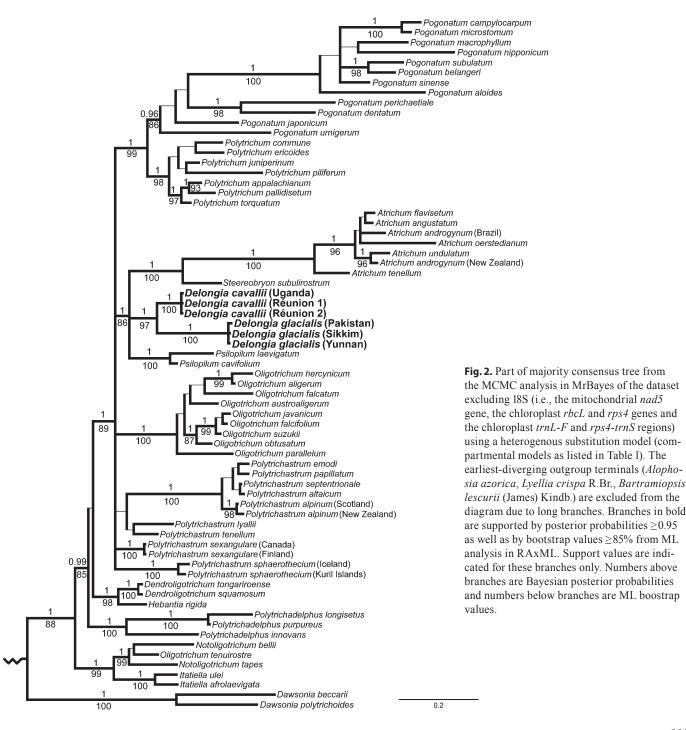
Topologies resulting from all three analytical methods (the optimal ML tree, the Bayesian majority consensus and the parsimony strict consensus) were compatible when derived from the same dataset, differing only in resolution. As in previous studies of Polytrichales (e.g., Bell & Hyvönen, 2010a), there was highly localised incongruence strongly supported by clade confidence metrics under all methods between analyses including and excluding 18S with regard to relationships between *Polytrichum*, the well-supported apical clade of *Pogonatum*, and the earlier-diverging *Pogonatum* species (*P. urnigerum* (Hedw.) P.Beauv., *P. dentatum* (Menzies ex Brid.) Brid., *P. perichaetiale* (Mont.) A.Jaeger, *P. japonicum* Sull. & Lesq.). However, these analyses were entirely congruent in their support for the relationships we are addressing here. In all analyses, a clade including all exemplars of *Oligotrichum* s.str. but excluding *O. cavallii* and *O. glaciale* had maximal support values (100% BS, 1.00 PP), while a clade grouping *O. cavallii* with *O. glaciale* was either maximally supported (in all Bayesian analyses) or strongly supported (ML BS = 93% and 97% including and excluding 18S respectively, parsimony BS = 92% and 95% including and excluding 18S). There were maximal support values in all analyses for the reciprocal monophyly of *O. cavallii* and *O. glaciale*. Furthermore, in analyses excluding 18S there were maximal or strong support values under both model-based methods for a clade including *Psilopilum*/*Steereobryon*/*Atrichum*/*Oligotrichum cavallii*/*O. glaciale* (PP = 1.00, BS = 86%), while under parsimony this clade was resolved but only with very low BS support (51%). For all analyses including 18S this clade was also

Table 1. Total number of characters, parsimony-informative characters and percentages of informative characters for each region used in the parsimony analyses, together with the optimal models selected for Bayesian analysis using the Akaike criterion within MrModeltest.

Region	Characters	Parsimony informative	%	Model
18S	1687	59	12	GTR+Γ+I
rbcL	580	69	14	GTR+Γ+I
rps4 gene	541	73	15	GTR+Γ+I
rps4-trnS	393	70	14	GTR+Γ
trnL-F	721	97	20	GTR+Γ+I
nad5 coding	864	50	10	HKY+Γ+I
nad5 intron	855	72	15	GTR+Γ+I

Table 2. Estimated marginal likelihoods obtained from path sampling for establishment of optimal substitution and tree process models to be used in BEAST analyses of dataset excluding 18S, with significance from Bayes factors calculated according to Kass & Raftery (1995).

Model	Marginal likelihood	2 log (B_{10}), significance
Yule	−14165.88	−12.56 (VS)
Birth-Death	−14159.60	**12.56 (VS)**
Homogenous	−14159.60	−6.52 (S)
Heterogenous	−14156.34	**6.52 (S)**

"Yule" = Yule process; "Birth-Death" = birth-death process; "Homogenous" = GTR+Γ+I substitution model applied to all compartments; "Heterogenous" = different substitution models applied as in Table 1. The final column lists Bayes factors as 2 log (B_{10}) together with significance (S = strong evidence; VS = very strong evidence and with the favoured model positive in bold). Path sampling was conducted using all potential calibration priors, i.e., including the *Eopolytrichum* fossil calibration. Tree process models were compared with the homogenous substitution model assumed, and the birth-death process was then assumed for substitution model comparison.

resolved, again with maximal support from Bayesian PP but only moderate support under ML (BS = 77%) and no support under parsimony. Within this clade, relationships between the *O. glaciale*/*O. cavallii* clade, *Psilopilum*, and the *Atrichum*/*Steereobryon* clade were unresolved under Bayesian and parsimony. Under ML analysis including 18S data the *O. glaciale*/*O. cavallii* clade was sister to *Atrichum* and *Steereobryon*, while with 18S excluded it was sister to *Psilopilum*, although in both cases there was no BS support value >50%. Figure 2 shows the Bayesian majority consensus tree from the analysis excluding 18S, with support values from both Bayesian PP and ML BS (for optimal

topologies from parsimony and ML analyses see Electr. Suppl.: Figs. S1 and S2, respectively).

There was no infraspecific variation in any of the sampled DNA regions for the three exemplars of *Oligotrichum cavallii*, while the *trnL-F* and *rps4* region sequences from a fourth exemplar from Mt. Kilimanjaro in Tanzania (not included in the analyses—see above and Bell & Hyvönen, 2012) also showed no variation. Within *O. glaciale*, all sampled regions were identical, except for a single synonymous substitution in *rbcL* present in the specimen from Pakistan. However, there were differences in all genomic regions between *O. cavallii*

Fig. 2. Part of majority consensus tree from the MCMC analysis in MrBayes of the dataset excluding 18S (i.e., the mitochondrial *nad5* gene, the chloroplast *rbcL* and *rps4* genes and the chloroplast *trnL-F* and *rps4-trnS* regions) using a heterogenous substitution model (compartmental models as listed in Table 1). The earliest-diverging outgroup terminals (*Alophosia azorica*, *Lyellia crispa* R.Br., *Bartramiopsis lescurii* (James) Kindb.) are excluded from the diagram due to long branches. Branches in bold are supported by posterior probabilities ≥0.95 as well as by bootstrap values ≥85% from ML analysis in RAxML. Support values are indicated for these branches only. Numbers above branches are Bayesian posterior probabilities and numbers below branches are ML boostrap values.

and *O. glaciale*. In total the species differed by three single–base pair substitutions in 18S, two in the 3′ segment of *rbcL*, five each in the *rps4* gene, the *rps4-trnS* intergenic spacer and the *nad5* intron, three in the *nad5* coding region, and seven in the *trnL-F* region. Additionally, the species differed by a single–base pair indel in the *rps4-trnS* intergenic spacer and, most significantly, a 96-bp indel in the *trnL* intron. The latter is due to *O. glaciale* (but not *O. cavallii*) sharing the highly reduced variant of the of the *trnL* intron P8 loop, also found in all members of *Oligotrichum* s.str. and nearly all *Pogonatum* species (see discussion in Bell & Hyvönen, 2010a).

Divergence time estimation. — Table 2 shows the results of the initial path sampling analyses comparing substitution and tree process models, while Table 3 shows estimated divergence times with 95% confidence intervals for the selected nodes resulting from the two differently calibrated final BEAST analyses, as well as estimated marginal likelihood values from path sampling and Bayes factor comparisons. A heterogenous substitution model with a birth-death tree process was favoured with strong or very strong evidence from Bayes factors (Table 2), and thus this general model was employed in the final analyses (Table 3). Estimates including a constrained minimum age of 80 million years on the MRCA of the *Polytrichum* clade based on the *Eopolytrichum* fossil are considerably older (80%–90%) than estimates calibrated without this constraint. However, Bayes factors from path sampling (Table 3) provide very strong evidence for rejecting this calibration. Confidence intervals for divergence times are wide in both cases, with most estimates overlapping at 95% confidence levels. The maximum clade credibility chronogram resulting from the analysis without the *Eopolytrichum* calibration is shown in Fig. 3.

Due to uncertainties surrounding assumptions inherent in the calibration priors we prefer to base our phylogeny estimation in this study on the results of the MrBayes and RAxML analyses (Fig. 2) rather than on relaxed-clock methods. Nonetheless it is worth noting that the topology implied by all moderate to high PP values for clades in the BEAST analysis is entirely consistent with those produced by the other methods and, in particular, that a *Delongia*/*Psilopilum* clade is supported at 69% PP (Fig. 3). This clade was resolved but without BS support in the corresponding RAxML analysis and had a posterior probability <50% in the MrBayes analysis, thus not appearing in the Bayesian majority consensus tree (Fig. 2).

Ancestral character state reconstruction. — The results of ancestral state reconstructions for reduction of leaf lamellae and leaf concavity are shown in Table 4. For the leaf lamellae character the MRCA of *Oligotrichum* s.str., *Delongia*, *Psilopilum*, *Atrichum* and *Steereobryon* is reconstructed as not having reduced lamellae (as defined above) with a probability of 0.71. The MRCAs of a *Delongia*/*Psilopilum*/*Atrichum*/*Steereobryon* group, a *Delongia* / *Psilopilum* group and *Delongia* itself are reconstructed as not having markedly concave leaves with probabilities of 0.79, 0.68 and 0.84 respectively.

Scanning electron microscopy. — Figure 4 shows SEM micrographs of apophyses and basal regions of capsules from *O. glaciale* and *Oligotrichum cavallii*, as well as representative micrographs of morphologies found in other potentially closely related species. In both *O. glaciale* and *O. cavallii*, the tissue in the apophysis is thick-textured and wrinkled and/or pitted in the dry state (Fig. 4A, B, F–H), causing many or most stomata to be recessed below the surface (they could be described as pseudocryptopore). In the moist state (as approximated by the fixed specimens subjected to CPD) most stomata are more or less superficial (Fig. 4C–E, I, J). By contrast,

Table 4. Posterior probabilities (PP) for reconstructed ancestral character states of leaf lamellae reduction and leaf concavity for MRCAs of selected groups of taxa, derived from analyses conducted using the "MultiState" option within BayesTraits.

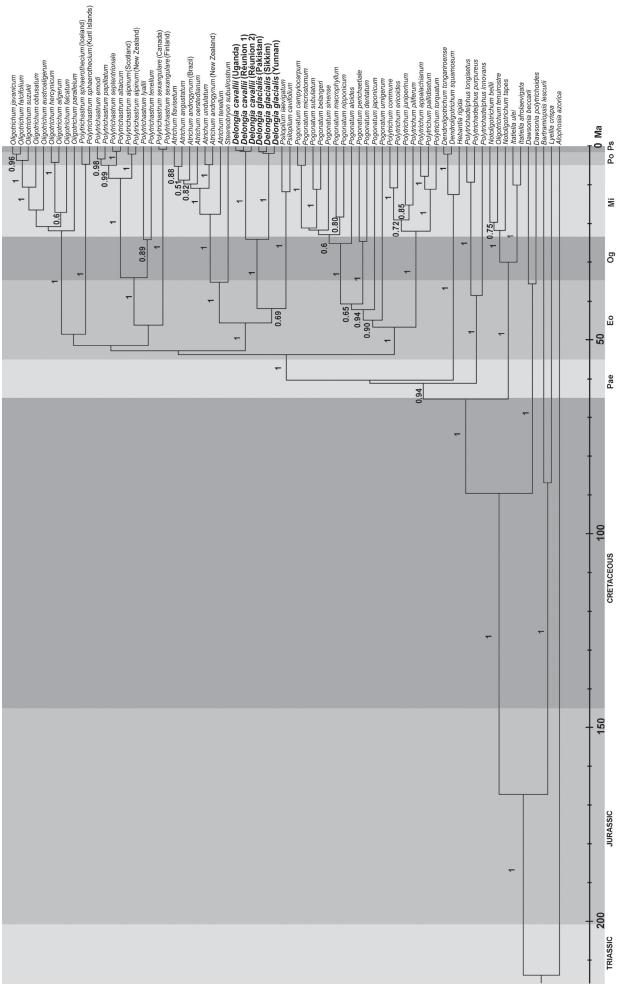| | Reconstructed character | | | |
| | Leaf lamellae | | Leaf concavity | |
Group for which MRCA state was reconstructed	Reduced	Not reduced	Not concave	Concave
Oligotrichum/*Delongia*/*Psilopilum*/ *Atrichum*/*Steereobryon*	0.29	**0.71**	–	–
Delongia/*Psilopilum*/ *Atrichum*/*Steereobryon*	–	–	**0.79**	0.21
Delongia/*Psilopilum*	–	–	**0.68**	0.32
Delongia	–	–	**0.84**	0.16

PPs for favoured states are in bold.

Table 3. Estimated divergence times for selected hypothesised clades from final uncorrelated lognormal relaxed-clock MCMC analyses implemented within BEAST, together with marginal likelihood values from path sampling and comparative Bayes factor significance for analyses conducted with and without the *Eopolytrichum* fossil calibration.

| | Estimated clade divergence times with 95% confidence intervals (Ma) | | | | |
Calibrations	*Delongia*	*Delongia*/*Psilopilum*	*Delongia*/*Psilopilum*/ *Atrichum*/*Steereobryon*	Marginal likelihood	2 log (B_{10}), significance
Including *Eopolytrichum*	22.58–**43.08**–67.39	53.75–**77.92**–101.96	68.28–**86.10**–105.48	−14156.34	−43.74 (VS)
Excluding *Eopolytrichum*	12.86–**23.23**–36.54	28.35–**41.11**–56.07	37.00–**45.20**–56.26	−14134.47	**43.74 (VS)**

Divergence time numbers in bold are geometric means of times and numbers in normal font are higher and lower 95% confidence intervals (highest posterior density intervals, HDP). Bayes factor significance is abbreviated as in Table 2 and the figure for the favoured calibration (positive) is in bold.

Fig. 3. Maximum clade credibility chronogram from BEAST relaxed-clock divergence time analysis of the dataset excluding 18S, with a substitution model as described for Fig. 2 and without using the calibration prior based on the *Eopolytrichum* fossil. Numbers on branches are posterior probabilities above 0.5. See Table 3 for 95% confidence intervals for nodes of interest. Mesozoic periods and Cenozoic epochs (abbreviated on scale bar) are in shades of grey.

representatives of *Oligotrichum* and *Psilopilum* have stomata of various types that are always superficial and the exothecium is not distinctly wrinkled or pitted (Fig. 4K–O).

Oligotrichum cavallii and *O. glaciale* differ in their morphologies and *O. cavallii* shows some variation in the form and positioning of individual stomata. In dry capsules of *O. glaciale* (assuming that the single slightly immature collection we have is representative) the stomata are associated with longitudinally orientated invaginations in the thick tissue of the apophysis, with the pores and guard cells mostly hidden below the surface of the exothecium (Fig. 4B). In the hydrated state

(as represented by specimens subjected to CPD) the apophysis tissue expands and the stomatal pores and guard cells become visible as the pockets in the spongy tissue are stretched out (Fig. 4D). The stomatal pores remain slightly recessed however, with the guard cells displaying a concave outer surface rather than bulging outwards as in most species (Fig. 4E; cf., e.g., *O. parallelum*, Fig. 4L). Although there is some variation in the degree to which individual stomata are recessed, and there are longer folds towards the base, the pattern is fairly regular.

Capsules of *Oligotrichum cavallii* show more irregular wrinkling of the apophysis, with longer, sometimes contorted,
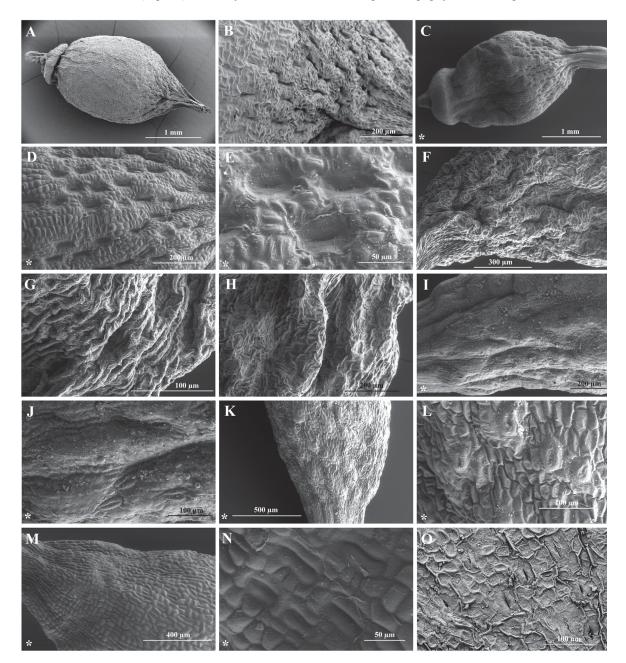

Fig. 4. Scanning electron micrographs of whole capsules and apophysis areas of *Delongia glacialis*, *D. cavallii* and selected related or potentially related taxa. Images with an asterisk in the bottom left corner are from specimens that were fixed and subjected to critical point drying to preserve the hydrated morphology, other images are from specimens prepared from dried material. **A–E,** *D. glacialis*; **F, I, J,** *D. cavallii* (specimen 1); **G, H,** *D. cavallii* (specimen 2); **K, L,** *Oligotrichum parallelum*; **M, N,** *Psilopilum cavifolium*; **O,** *O. obtusatum*. Voucher specimens are listed in Appendix 2.

infolded fissures in the dry state (Fig. 4F) that do not completely disappear in the hydrated state (Fig. 4I). Moreover, the positioning of the stomata is more random with respect to the topology of the apophysis. Although many stomata occur at the bases of fissures or pits and are thus hidden in the dry state and exposed in the hydrated state, others remain superficial even in the dry state (Fig. 4F–H, J).

■ **DISCUSSION**

Phylogeny, morphology and evolution. — Our molecular results strongly support *Oligotrichum cavallii* and *O. glaciale* as sister species and indicate that they share a more recent common ancestor with *Psilopilum*, *Steereobryon* and *Atrichum* than with

other members of *Oligotrichum*. Their gametophyte morphologies are compatible with this while their sporophyte morphologies tentatively unite them by features not found in any other *Oligotrichum* species. Ecologically, both are plants of mountain habitats, while representing quite distinct lineages with strongly divergent morphologies and widely separated distributions. *Oligotrichum cavallii* occurs across the Western and Eastern Rift mountains in East Africa and also on Réunion, while *O. glaciale* spans the Himalaya from Pakistan to Yunnan (Fig. 1). Based on our limited but wide-ranging sampling both species are remarkably uniform genetically, suggesting a history of recent frequent dispersal within their respective ranges and probably also a relatively recent population bottleneck in each case.

Oligotrichum cavallii is unusual in *Oligotrichum* s.str. (Bell & Hyvönen, 2012) in having coarsely serrate leaf margins
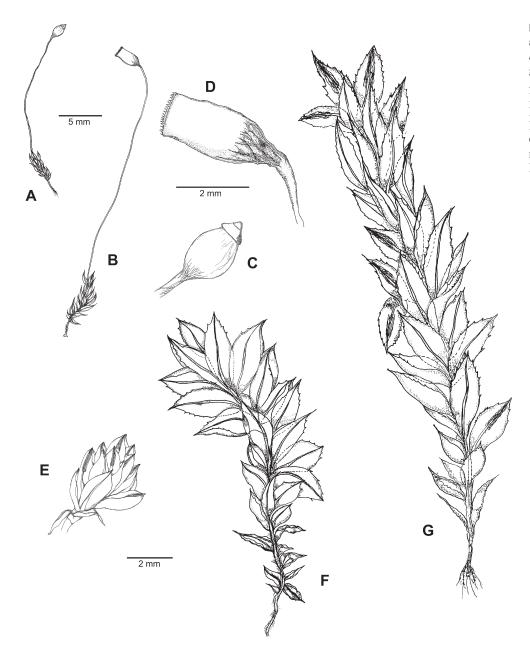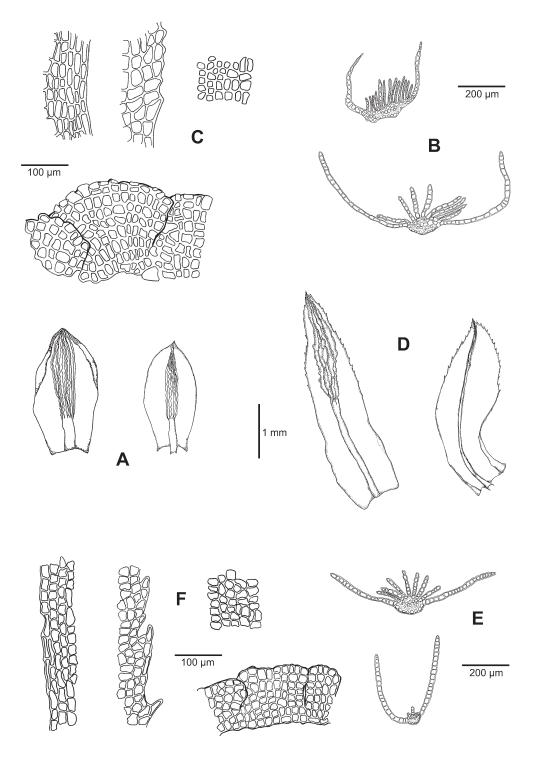

Fig. 5. *Delongia glacialis* **(A, C, E)** and *D. cavallii* **(B, D, F, G).** **A, B,** whole plants; **C, D,** sporangia; **E–G,** gametophyte stems. — A, C = *Long 22696* (Sikkim); E = *Long 24132* (Yunnan); B, D = *Townsend 85/290* (Kenya), F = *Hedderson 17893* (Réunion), G = *Pócs 6788/AD* (Mt. Kilimanjaro). — Drawn by Isuru U. Kariyawasam.

with large, acute, distinctly multicellular teeth (Figs. 5F, G, 6D, F); this is otherwise seen only in *O. parallelum*, the likely sister species to the rest of *Oligotrichum*. Also, in common only with *O. glaciale, O. falcatum* Steere, *O. falcifolium* (Griff.) G.L.Sm., *O. obtusatum* and *O. semilamellatum* (Hook.f.) Mitt., it lacks any distinct lamellae on the abaxial lamina (Fig. 6E), although there are usually two or three large teeth or spines on the back of the costa towards the apex and one specimen we have seen also has a few short spines on the back of the

apical lamina. Originally described under *Catharinea* Ehrh. ex F.Weber & D.Mohr (≡ *Atrichum*), robust forms with more lingulate-lanceolate leaves, shorter adaxial lamellae and well-developed, acute marginal toothing may indeed superficially resemble *Atrichum*. Although the lack of a differentiated margin as well as capsule morphology clearly separate it from *Atrichum*, there is a tendency towards elongation of the outermost marginal row of cells towards the leaf bases in many specimens that hints at affinities with this genus and with *Psilopilum* (Figs. 5D,

Fig. 6. *Delongia glacialis* **(A, B, C)** and *D. cavallii* **(D, E, F). A, D,** vegetative leaves; **C, F,** basal marginal cells (left), median to upper marginal cells, median laminal cells and lamellae in side view; **B, E,** leaf transverse sections. — A (left), B (upper), C (marginal cells) = *Townsend 89/456* (Kashmir); A (right) = *Long 17088* (Nepal); B (lower), C (median lamina cells and lamella) = *Townsend 89/401*; D (left), F (median lamina cells and lamella), E (upper) = *Pócs 6788/ AD* (Mt. Kilimanjaro); D (right), E (lower), F (marginal cells) = *Hedderson 17893* (Réunion). — Drawn by Isuru U. Kariyawasam and Neil E. Bell.

6F), while the outermost one or two rows of cells in the upper lamina often have cell walls that are more strongly coloured and occasionally very slightly more incrassate. In fact the species is highly variable gametophytically, especially in the size, shape and habit of the leaves and the degree of development of the lamellae. The collections from Réunion in particular are extremely disparate, with one specimen having fairly long stems (>15 mm) and rather broad, lax leaves with highly reduced lamellae (one to three cells high or completely absent; Fig. 6D right, 6E lower picture), and the other with much shorter stems and resembling a poorly grown example of plants from the Western Rift Mountains in mainland Africa, which have more ovate-lanceolate leaves and well developed, strongly undulate lamellae. The material we have from Mt. Elgon in Uganda is of this type and closely resembles the illustration in De Sloover (1979) of his collection *13689* from Rwanda. The specimens we have seen from Mt. Kilimanjaro (Eastern Rift Mountains) on the other hand (Figs. 5G, 6D left, 6E upper picture) are extremely robust, with a fairly lax habit and stems up to 5 cm long, more lanceolate-lingulate leaves and with the lamellae moderately well developed. In general, variation within the species is between plants with laxer, flatter-margined, more obtuse leaves that are strongly twisted when dry and have less well developed lamellae, and ones with more lanceolate upper leaves that are less altered when dry and have erect upper lamina margins and more strongly developed lamellae (it is on an extreme form of this latter type that we have observed short spines on the abaxial lamina). Given this variability, and the isolated nature of individual populations, the lack of any differentiation in our molecular markers is surprising, especially as our molecular sampling spanned the range of morphological variation fairly comprehensively. As the highly divergent forms from Réunion were found very close to each other and with the laxer form in deep shade, it seems likely that a significant amount of variation results from a high degree of phenotypic plasticity.

Oligotrichum glaciale shares with *O. cavallii* the lack of abaxial lamellae and further seems to lack any spines on the apical costa or lamina, while the strongly undulate adaxial lamellae resemble those found in forms of *O. cavallii* that have well-developed lamellae (Fig. 6A–C). The combination of strongly undulate adaxial lamellae with a lack of abaxial lamellae is unusual in *Oligotrichum*, being otherwise found only in *O. cavallii* and in some forms of *O. falcatum*. However, in forms of *O. cavallii* with very reduced lamellae these are less distinctly undulate. Otherwise *O. glaciale* has a very different morphology from *O. cavallii* and from all other *Oligotrichum* species, with broadly ovate, obtuse, highly concave leaves that are mostly only slightly dentate to entire and closely resemble those of *Psilopilum* (Fig. 6A, C). The lack of any differentiation of the lower marginal leaf cells and the morphology of the sporophyte clearly separate *O. glaciale* from *Psilopilum*, however, while our ancestral state reconstructions indicate that the highly concave leaf form is likely to be independently derived in the two taxa. As mentioned above, *O. cavallii* does sometimes show some "*Psilopilum*-like" elongation of the marginal cells towards the leaf base (Fig. 6F), although otherwise its leaf morphology is very different from that of *Psilopilum*.

The morphology of the sporophyte, and the apophysis in particular, unite *Oligotrichum glaciale* and *O. cavallii*, despite a unique expression in each species. In *O. cavallii* the peristome is composed almost entirely of simple teeth and there are notably more than 32 (usually around 40 in the small number of specimens we have seen). Although a few irregularly compound teeth may be present these are rarely fully united. This contrasts with *Oligotrichum* s.str., in which many species have 32 exclusively and regularly compound teeth (e.g., *O. parallelum*, *O. aligerum*), while others (e.g., *O. falcatum*, *O. hercynicum*, *O. crossidioides* P.C.Chen & T.L.Wan ex W.X.Xu & R.L.Xiong) have an irregular mixture of multiple compound and some simple teeth (still always around 32 or slightly fewer). It is difficult to observe the peristome in our fertile material of *O. glaciale* due to nearly all of the capsules being at a pre-dehiscent stage, but from dissection of these as well as observation of the one or two old capsules present (unfortunately not in good condition), it appears that this species has a rather irregular peristome with a high basal membrane and short, acute, peg-like teeth that are (at least predominantly) simple, as in *O. cavallii*. Unlike in *O. cavallii*, however, the number of teeth would appear to be less than 32.

Both *Oligotrichum glaciale* and *O. cavallii* seem to have well-developed "spongy" tissue at the base of the capsule that is invaginated when dry and expanded when wet, causing at least some stomata to be obscured in the dry state. In *O. glaciale* there is a clear one-to-one association between stomata and individual invaginations or pockets, while in *O. cavallii*, although some stomata are individually recessed (Fig. 4G), others occur multiply at the bases of elongated folds (Fig. 4F, J) while yet others are entirely superficial (Fig. 4H, J). Caution is perhaps warranted in the case of *O. glaciale*, as the only known fertile material has capsules that are not quite fully mature. It is conceivable that in the fully developed state the stomata could be superficial when both dry and hydrated and that the external morphology of the guard cells could be different. In any case, a thick-textured apophysis with some stomata obscured in the dry state is synapomorphic for the two species, with this general type of morphology being unusual and not found in any other taxa sampled for this study. Recessed stomata in vascular plants are often associated with water retention in xeric environments (e.g., Benzing, 1990). As the hydration state of the capsule is likely to reflect changes in water availability, it is possible that a mechanism causing stomatal exposure to vary with hydration could be beneficial in exposed mountain environments where dry, cold winds are a major factor in transient desiccation. We would expect this to be most significant during the period of maximum photosynthetic activity of the capsule, i.e., prior to full maturity and meiosis (Proctor, 1977). To put these speculations on a more secure footing, however, it would be necessary to confirm that such dynamic responses to hydration occurred in vivo, and at developmental stages when photosynthetic activity in the sporophyte was significant.

While a significant number of independent molecular characters underlie the strong support in the phylogenetic analyses for the monophyly of *Oligotrichum cavallii* + *O. glaciale*, a useful diagnostic synapomorphy for the clade is provided by

the occurrence of histidine at amino acid position 143 of the *rps4* gene, represented by the codon CAC. Without exception, and based on our extensive sampling from all genera (e.g., Bell & Hyvönen, 2010a), all other known Polytrichaceae have glutamine at this position, coded by CAA.

Both morphology and tentative (but never convincing) evidence from some previous molecular studies (e.g., Bell & Hyvönen, 2010a) would be compatible with viewing *Oligotrichum* s.str. and the *Psilopilum*/*Steereobryon*/*Atrichum*/*O. cavallii*/*O. glaciale* clade as sister groups. However this relationship is not consistently supported here, appearing in the single optimal ML tree but with bootstrap support less than 50%, and present in less than 50% of the topologies sampled in the Bayesian analyses. The latter may explain the failure of Bayesian ancestral character state reconstruction to favour reduced lamellae as the ancestral condition of the MRCA of these two groups. The maximum clade credibility tree from the divergence time analysis (Fig. 3) groups *Oligotrichum* s.str. and *Polytrichastrum sphaerothecium* as sister to the core *Polytrichastrum* clade, but with no PP support values above 50% for the relevant nodes. In any case, the common ancestor of the *Psilopilum*/*Steereobryon*/*Atrichum*/*O. cavallii*/*O. glaciale* clade presumably had an *Oligotrichum*-like gametophyte morphology (whether homologous with *Oligotrichum* s.str. or independently evolved), with the unique *Atrichum* type being derived. This is potentially consistent with the conspicuously long branch in our non-chronological topologies corresponding to accelerated rates of molecular evolution in the *Atrichum* lineage (also seen in *Pogonatum*, another morphologically highly derived group; see Fig. 2). Although relationships between genotypic and phenotypic change are controversial and the neutral theory (Kimura, 1983) predicts independence, some studies suggest limited correlation in plants specifically (Davies & Savolainen, 2006), while others appear to show a clear relationship when functional genes such as *rbcL* are considered (e.g., Bousquet & al., 1992). Similarly, the mutually very distinct sporophyte morphologies of *Psilopilum*, *Atrichum* and the *O. glaciale*/*O. cavallii* clade are likely to be derived from a more generalised type. From a taxonomic perspective the retention of many of the same plesiomorphic characters in *O. cavallii* and *O. glaciale*, together with the many autapomorphies that so clearly separate the species from each other, makes for a less morphologically discrete generic-level grouping than is ideal, but the molecular evidence for such a group is robust and the alternative of recognising each species as a monotypic genus seems nomenclaturally profligate. It would also clearly be highly unsatisfactory (even if support values justified it) to expand the current concept of *Oligotrichum* to include species of *Psilopilum*, *Atrichum* and *Steereobryon*. Our solution (below) is compatible with the recommendations of authors such as Wiley & al. (1991) in requiring the smallest number of taxonomic changes.

Divergence time estimation. — The relative lack of information for calibrating our divergence time estimates is reflected in fairly wide confidence intervals (Table 3), while the *Eopolytrichum* fossil calibration has an extreme effect on estimated MRCA dates and thus appears at odds with the other

assumptions. This is corroborated by Bayes factors, which very strongly favour the analysis calibrated without the *Eopolytrichum* prior (chronogram in Fig. 3). This is perhaps not surprising given the fossil's puzzling combination of sporophyte characters and poorly supported phylogenetic position (Hyvönen & al., 2004). With the recent expansion of *Polytrichum* to include species previously placed in *Polytrichastrum* sect. *Aporotheca* (Limpr.) G.L.Merr. (Bell & Hyvönen, 2010b), *Eopolytrichum* should hypothetically now be accommodated within *Polytrichum* if its position in the phylogenetic analyses of Hyvönen & al. (2004) is accepted. The latter derives from its possession of a "discoid" apophysis, a mamillose, pitted exothecium and echinulate spores, these features being absent in *Polytrichum* sect. *Aporotheca*. However, its other characters (see Materials and Methods) sit extremely uneasily within *Polytrichum* and challenge this placement. Interestingly, the statistical support from Bayes factors in the current study for the analysis excluding a calibration based on this placement could be seen as reducing confidence in the phylogenetic placement itself (as an assumption that results in a significantly lower marginal likelihood).

If the results deriving from the analysis excluding the *Eopolytrichum* fossil calibration are favoured on the above grounds, then divergence time estimates (Table 3) indicate that the lineages represented by the extant *Oligotrichum glaciale* and *O. cavallii* diverged from each other no later than the Middle Miocene (~13 Ma), no earlier than the late Oligocene (~37 Ma) and most probably around the Oligocene-Miocene boundary (~23 Ma). They most likely share a common ancestor with *Psilopilum*, *Atrichum* and *Steereobryon* in the Eocene (~56–34 Ma). Whether or not the *O. glaciale*/*O. cavallii* clade is sister to *Psilopilum* (as seems marginally more likely) or to *Atrichum* and *Steereobryon*, the divergence of the *O. glaciale*/*O. cavallii* clade from its sister group was probably also in the Eocene, relatively soon after the initial divergence from the more distantly related lineage. We do, however, acknowledge the multiple uncertainties inherent in divergence time estimations (as critically discussed, for example, by Sauquet & al., 2012 and Wheeler, 2012). For example, the calibration based on the estimated age of Polytrichales taken from Newton & al. (2007) relies on the validity of the assumptions made in that study, which used different methods and phylogenetically distant fossil calibrations. We are aware of two polytrichaceous fossils that remain unpublished, the use of which as calibration points may eventually allow critical re-evaluation of the estimates presented here.

Biogeography. — The strongly disjunct distribution ranges of *Oligotrichum glaciale* and *O. cavallii* are interesting, especially as both occur in mountain environments and seem (from their limited infraspecific molecular variation) able to disperse over long distances between ecologically isolated habitats within their respective ranges. It is likely that adaptations to geological factors (bedrocks and associated soils), closely coupled with possible adaptations to high-altitude environments, played a significant role in their differentiation and have an ongoing role in keeping their distributions well separated. The mountain ranges in Africa and Réunion where *O. cavallii* occurs are exclusively volcanic, while the Himalaya are predominantly

composed of sedimentary and metamorphic rocks. Furthermore, *O. glaciale* occurs at higher altitudes than *O. cavallii* and in more open habitats. Hypothesised divergence times for the *O. glaciale* and *O. cavallii* lineages are contemporaneous with the origins of the East African Rift system and ongoing uplift of the Qinghai-Tibetan Plateau, arguing against a recent origination of the clade in one of these regional ecosystems followed by dispersal to the other. More probable is that the two extant species represent regionally adapted relicts of a previously more widespread group of species.

Interestingly, the combination of evident adaptations to volcanic substrates with adaptations to specific climatic conditions appears to explain the distribution of another relatively small, largely montane polytrichaceous species. *Polytrichastrum sphaerothecium* is found only on volcanic rock in cool oceanic areas, thus explaining its peculiar disjunct distribution between Japan, N.E China, the Aleutian and Kuril Islands, and Iceland, while infraspecific molecular variation similarly hints at little or no reproductive isolation between Icelandic and East Asian populations (Bell & Hyvönen, 2010a). *Polytrichastrum* also contains two high-altitude Himalayan endemic species, *P. emodi* G.L.Sm. and *P. papillatum* G.L.Sm. (Smith, 1974).

Taxonomic conclusions. — Here we erect *Delongia* gen. nov. to accommodate *Oligotrichum glaciale* and *O. cavallii*. The genus is named in honour of David Long, recently retired after four decades of outstanding bryological work at the Royal Botanic Garden, Edinburgh. As well as being an expert on the Himalayan bryoflora he authored the treatment of the Polytrichaceae for the *Illustrated moss flora of arctic North America and Greenland*. He was instrumental in developing the early bryological careers of the first two authors as supervisor of their M.Sc. projects (both on Polytrichaceae, in 1999 and 2013 respectively), and his Himalayan collections were of considerable importance for the fourth author in his studies of the family. His collections of *O. glaciale* from Sikkim, Nepal and Yunnan were a critical resource for this project and remain the only known specimens from outside of the general type locality of Kashmir.

■ TAXONOMY

Delongia N.E.Bell, Kariyawasam, Hedd. & Hyvönen, **gen. nov.** – Type: *Delongia glacialis* (C.C.Towns.) N.E.Bell, Kariyawasam, Hedd. & Hyvönen (≡ *Oligotrichum glaciale* C.C.Towns.).

Diagnosis. – Sporophytes with thick-textured, wrinkled or pitted apophysis and simple peristome teeth (a few irregularly compound teeth may be present). Gametophyte stems generally unbranched, naked with rhizoids at extreme base only. Leaves lacking abaxial lamellae (may have short spines on back of costa towards apex or occasionally on back of lamina) and with strongly undulate adaxial lamellae restricted to the costa. Distinct leaf border not present. Leaves either strongly concave (in which case marginal row of cells not elongated towards base) or else with prominent multicellular teeth towards apex. Calyptra cucullate, only slightly roughened at tip or with a very

few isolated short hairs. Histidine at amino acid position 143 of subunit four of the chloroplast small ribosomal protein (codon = CAC).

Delongia glacialis (C.C.Towns.) N.E.Bell, Kariyawasam, Hedd. & Hyvönen, **comb. nov.** ≡ *Oligotrichum glaciale* C.C.Towns. in J. Bryol. 20: 52, fig. 2. 1998 – Holotype: India, Kashmir, Rasbal [34°25′N, 75°00′E], ca. 3800 m, at the edge of melting snow below crags above the stream, 9 Aug 1989, *Townsend 89/401* (E barcode E00049314!).

Abbreviated Description (for full description, see Electr. Suppl.: Appendix S1). – Plants mostly small. Erect *stems* (0.3)0.5–1.0(1.9) cm tall. *Leaves* broad, (1.3)l.5–2.3(2.7) mm long, 0.7–1.3(2.0) mm wide, usually extremely concave, obtuse. Leaf bases narrowed but hardly differentiated, not distinctly sheathing. *Costa* strong, ending abruptly immediately before extreme apex, abaxial teeth not present. *Margin* undifferentiated, entire or denticulate to weakly dentate towards apex. Abaxial lamellae and spines absent. *Adaxial lamellae* (3)6–8(12), restricted to costa, (4)6–10 cells high, undulate to profoundly and sharply undulate longitudinally; end cells not significantly differentiated. *Mid lamina cells* quadrate to hexagonal or irregularly isodiametric, not markedly incrassate, (13)l7–25(30) μm. Basal cells mostly rectangular, around the same width as mid lamina cells, 1–5× as long as wide. *Male plants* small and composed mostly of bud-like perigonium. *Sporophytes* with seta 1.5–3 cm long, straight or variously sinuose; capsules more or less orthotropous, 2–3 mm long, ovoid, terete, symmetrical, lower half to third composed of thick-textured apophysis in which numerous stomata appear to be recessed in pits in the dry state and exposed in the moist state. Operculum shortly rostrate. Peristome only observed in predehiscent and in very old capsules; apparently somewhat reduced with high basal membrane and less than 32 (around 25?) simple, peg-like teeth. *Calyptrae* only seen in packet; cucullate, roughened at tip, apparently without hairs.

Delongia cavallii (G.Negri) N.E.Bell, Kariyawasam, Hedd. & Hyvönen, **comb. nov.** ≡ *Catharinea cavallii* G.Negri in Ann. Bot. (Rome) 7: 168. 1908 ≡ *Oligotrichum cavallii* (G.Negri) G.L.Sm. in Mem. New York Bot. Gard. 2l(3): 53. 1971 – Type: Africa, Ruwenzori, Bujongolo, 3800 m, *Negri s.n.* (not located).

Abbreviated Description (for full description, see Electr. Suppl.: Appendix S1). – Plants very variable in size and habit. *Stems* erect, generally from (0.7)l.0 to 2.5 cm but sometimes up to 5 cm. *Leaves* variable, from long-elliptical or slightly spathulate with sub-acute apices to ovate-lanceolate with acute apices; (2.0)3.0–3.5(4) cm long, (0.6)0.8–1.2(1.5) cm wide at broadest point. Leaf bases only slightly differentiated on vegetative leaves, weakly sheathing. *Costa* variable but generally fairly narrow, ending abruptly immediately before extreme apex, with a few coarse teeth or spines abaxially towards apex. *Margin* undifferentiated or only very vaguely differentiated; coarsely toothed with large, acute, distinctly multicellular teeth from around midleaf. Abaxial lamellae absent, rarely a few scattered spines on abaxial lamina towards apex. *Adaxial lamellae* highly variable, from 2 to 3 and only 1–3 cells high

or effectively absent, to up to 8 or 9 and up to 10 cells high, restricted to costa, undulate to profoundly and sharply undulate longitudinally when well developed, laterally with upper margin undulate, end cells not significantly differentiated. *Mid lamina cells* quadrate-hexagonal to irregularly isodiametric, fairly thin-walled, fairly variable in size between specimens, (13)15–28(32) µm. Basal cells rectangular, around the same width as mid lamina cells, 1–4× as long as wide. *Male Plants* slightly shorter than female plants with apical, bud like perigonium. *Sporophytes* with seta 2–3.5 cm long, straight or variously sinuose; capsules mostly homotropous (sub-orthotropous to sub-orthogonal), 3–5 mm long, short-cylindric, terete, symmetrical, lower portion composed of thick-textured apophysis with multiple, more or less contorted wrinkles that are more prominent when dry, stomata scattered on apophysis, some superficial and others partially concealed inside wrinkles. Operculum shortly rostrate or acutely conical. Peristome composed almost entirely of simple teeth, widely separated and obtusely lanceolate, irregular in number but approximately 40, a few compound or semi-compound teeth sometimes present. *Calyptrae* only seen in packet; cucullate, roughened at tip and with a very few isolated, short hairs.

■ ACKNOWLEDGEMENTS

■ LITERATURE CITED

Akaike, H. 1974. A new look at the statistical model identification. *IEEE Trans. Automatic Control* 19: 716–723. http://dx.doi.org/10.1109/TAC.1974.1100705

Baele, G., Lemey, P., Bedford, T., Rambaut, A., Suchard, M.A. & Alekseyenko, A.V. 2012. Improving the accuracy of demographic and molecular clock model comparison while accommodating phylogenetic uncertainty. *Molec. Biol. Evol.* 29: 2157–2167. http://dx.doi.org/10.1093/molbev/mss084

Beckert, S., Steinhauser, S., Muhle, H. & Knoop, V. 1999. A molecular phylogeny of bryophytes based on nucleotide sequences of the mitochondrial *nad5* gene. *Pl. Syst. Evol.* 218: 179–192. http://dx.doi.org/10.1007/BF01089226

Beckert, S., Muhle, H., Pruchner, D. & Knoop, V. 2001. The mitochondrial *nad2* gene as a novel marker locus for phylogenetic analysis of early land plants: A comparative analysis in mosses. *Molec. Phylogen. Evol.* 18: 117–126. http://dx.doi.org/10.1006/mpev.2000.0868

Bell, N.E. & Hyvönen, J. 2008. Rooting the Polytrichopsida: The phylogenetic position of *Atrichopsis* and the independent origin of the polytrichopsid peristome. Pp. 227–239 in: Mohamed, H., Baki, B.B., Nasrulhaq-Boyce, A. & Lee, P.K.Y. (eds.), *Bryology in the New Millennium*. Kuala Lumpur: University of Malaya.

Bell, N.E. & Hyvönen, J. 2010a. Phylogeny of the moss class Polytrichopsida (Bryophyta): Generic-level structure and incongruent gene trees. *Molec. Phylogen. Evol.* 55: 381–398. http://dx.doi.org/10.1016/j.ympev.2010.02.004

Bell, N.E. & Hyvönen, J. 2010b. A phylogenetic circumscription of *Polytrichastrum* (Polytrichaceae): Reassessment of sporophyte morphology supports molecular phylogeny. *Amer. J. Bot.* 97: 566–578. http://dx.doi.org/10.3732/ajb.0900161

Bell, N.E. & Hyvönen, J. 2012. Gametophytic simplicity in Laurasian and Gondwanan Polytrichopsida — The phylogeny and taxonomy of the *Oligotrichum* morphology. *J. Bryol.* 34: 160–172. http://dx.doi.org/10.1179/1743282012Y.0000000015

Bell, N.E., Quandt, D., O'Brien, T.J. & Newton, A.E. 2007. Taxonomy and phylogeny in the earliest diverging pleurocarps: Square holes and bifurcating pegs. *Bryologist* 110: 533–560. http://dx.doi.org/10.1639/0007-2745(2007)110[533:TAPITE]2.0.CO;2

Benzing, D.H. 1990. *Vascular epiphytes: General biology and related biota*. Cambridge: Cambridge University Press. http://dx.doi.org/10.1017/CBO9780511525438

Bouckaert, R., Heled, J., Kühnert, D., Vaughan, T.G., Wu, C.-H., Xie, D., Suchard, M.A., Rambaut, A. & Drummond, A.J. 2014. BEAST2: A software platform for Bayesian evolutionary analysis. *PLoS Computat. Biol.* 10: e1003537. http://dx.doi.org/10.1371/journal.pcbi.1003537

Bousquet, J., Strauss, S.H. & Li, P. 1992. Complete congruence between morphological and *rbcL*-based molecular phylogenies in birches and related species (Betulaceae). *Molec. Biol. Evol.* 9: 1076–1088.

Capesius, I. & Stech, M. 1997. Molecular relationships within mosses based on 18S rRNA gene sequences. *Nova Hedwigia* 64: 525–533.

Davies, T.J. & Savolainen, V. 2006. Neutral theory, phylogenies, and the relationship between phenotypic change and evolutionary rates. *Evolution* 60: 476–483. http://dx.doi.org/10.1111/j.0014-3820.2006.tb01129.x

De Sloover, J.L. 1979. Note de bryologie africaine. *Bull. Jard. Bot. Natl. Belg.* 56: 241–300. http://dx.doi.org/10.2307/3668193

Drummond, A.J. & Rambaut, A. 2007. Beast: Bayesian evolutionary analysis by sampling trees. *B. M. C. Evol. Biol.* 7: 214. http://dx.doi.org/10.1186/1471-2148-7-214

Drummond, A.J., Ho, S.Y.W., Phillips, M.J. & Rambaut, A. 2006. Relaxed phylogenetics and dating with confidence. *PLoS Biol.* 4: 699–710. http://dx.doi.org/10.1371/journal.pbio.0040088

Ellis, L.T., Bayliss, J., Bruggeman-Nannenga, M.A., Cykowska, B., Ochyra, R., Gremmen, N.J.M., Frahm, J.-P., Hedderson, T.A., Heras, P., Infante, V.M., Hugonnot, V., Mogro, F., Plášek, V., Číhal, L., Sawicki, J., Schäfer-Verwimp, A., Stebel, A., Ştefănuţ, S., Váňa, J., Yang, J.-D. & Lin, S.-H. 2014. New national and regional bryophyte records, 38. *J. Bryol.* 36: 61–72. http://dx.doi.org/10.1179/1743282013Y.0000000085

Farris, J.S. 1989. The retention index and the rescaled consistency index. *Cladistics* 5: 417–419. http://dx.doi.org/10.1111/j.1096-0031.1989.tb00573.x

Farris, J.S., Albert, V.A.A., Källersjö, M., Lipscomb, D. & Kluge, A.G. 1996. Parsimony jackknifing outperforms neighbor joining. *Cladistics* 12: 99–124. http://dx.doi.org/10.1111/j.1096-0031.1996.tb00196.x

Frahm, J.-P. 2004. *Atrichum* (Musci, Polytrichaceae) in Baltic amber. *J. Hattori Bot. Lab.* 95: 219–227.

Gaut, B.S. 1998. Molecular clocks and nucleotide substitution rates in higher plants. *Evol. Biol.* 30: 93–120. http://dx.doi.org/10.1007/978-1-4899-1751-5_4

Gelman, A. & Meng, X.L. 1998. Simulating normalizing constants: From importance sampling to bridge sampling to path sampling. *Statist. Sci.* 13: 163–185. http://dx.doi.org/10.1214/ss/1028905934

Gernhard, T. 2008. The conditioned reconstructed process. *J. Theor. Biol.* 253: 769–778. http://dx.doi.org/10.1016/j.jtbi.2008.04.005

Goloboff, P.A. 1994. Nona: A tree-searching program, version 2.0. http://www.cladistics.com/aboutNona.htm

Goloboff, P.A., Farris, J.S. & Nixon, K.C. 2003. TNT: Tree analysis using new technology, version 1.1. http://www.lillo.org.ar/phylogeny/tnt/

Goloboff, P.A., Farris, J.S. & Nixon, K.C. 2008. TNT, a free program for phylogenetic analysis. *Cladistics* 24: 774–786. http://dx.doi.org/10.1111/j.1096-0031.2008.00217.x

Hyvönen, J., Hedderson, T.A., Smith Merrill, G.L., Gibbings, J.G. & Koskinen, S. 1998. On phylogeny of the Polytrichales. *Bryologist* 101: 489–504. http://dx.doi.org/10.1639/0007-2745(1998)101[489:OPOTP]2.0.CO;2

Hyvönen, J., Koskinen, S., Smith Merrill, G.L., Hedderson, T.A. & Stenroos, S. 2004. Phylogeny of the Polytrichales (Bryophyta) based on simultaneous analysis of molecular and morphological data. *Molec. Phylogen. Evol.* 31: 915–928. http://dx.doi.org/10.1016/j.ympev.2003.11.003

Kass, R.E. & Raftery, A.E. 1995. Bayes factors. *J. Amer. Statist. Assoc.* 90: 773–795. http://dx.doi.org/10.1080/01621459.1995.10476572

Kelchner, S.A. 2000. The evolution of non-coding chloroplast DNA and its application in plant systematics. *Ann. Missouri Bot. Gard.* 87: 482–498. http://dx.doi.org/10.2307/2666142

Kimura, M. 1983. *The neutral theory of molecular evolution.* Cambridge: Cambridge University Press. http://dx.doi.org/10.1017/CBO9780511623486

Kluge, A.G. & Farris, J.S. 1969. Quantitative phyletics and the evolution of Anurans. *Syst. Zool.* 18: 1–32. http://dx.doi.org/10.2307/2412407

Konopka, A.S., Herendeen, P.R., Smith Merrill, G.L. & Crane, P.R. 1997. Sporophytes and gametophytes of Polytrichaceae from the Campanian (late Cretaceous) of Georgia, USA. *Int. J. Pl. Sci.* 158: 489–499. http://dx.doi.org/10.1086/297459

Merced, A. & Renzaglia, K. 2013. Moss stomata in highly elaborated *Oedipodium* (Oedipodiaceae) and highly reduced *Ephemerum* (Pottiaceae) sporophytes are remarkably similar. *Amer. J. Bot.* 100: 2318–2327. http://dx.doi.org/10.3732/ajb.1300214

Müller, J., Müller, K.F., Neihuis, C. & Quandt, D. 2011. PhyDE: Phylogenetic data editor, version 0.997. http://phyde.de

Newton, A.E., Wikström, N., Bell, N.E., Forrest, L.L. & Ignatov, M.S. 2007. Dating the diversification of the pleurocarpous mosses. Pp. 329–358 in: Newton, A.E. & Tangney, R. (eds.), *Pleurocarpous mosses: Systematics and evolution.* Systematics Association Special Volume Series 71. Boca Raton: CRC Press. http://dx.doi.org/10.1201/9781420005592

Nixon, K.C. 2002. WinClada, version 1.00.08. http://www.cladistics.com/aboutWinc.htm

Nylander, J.A.A. 2004. MrModeltest, version 2.2. http://abc.se/~nylander/

Ogata, Y. 1989. A Monte Carlo method for high dimensional integration. *Numer. Math.* 55: 137–157. http://dx.doi.org/10.1007/BF01406511

Pagel, M. & Meade, A. 2006. Bayesian analysis of correlated evolution of discrete characters by reversible-jump Markov chain Monte Carlo. *Amer. Naturalist* 167: 808–825. http://dx.doi.org/10.1086/503444

Pagel, M., Meade, A. & Barker, D. 2004. Bayesian estimation of ancestral character states on phylogenies. *Syst. Biol.* 53: 673–684. http://dx.doi.org/10.1080/10635150490522232

Palmer, J.D. 1991. Plastid chromosome, structure and evolution. Pp. 5–53 in: Bogorad, L. & Vasil, I.K. (eds.), *The molecular biology of plastids.* San Diego: Academic Press. http://dx.doi.org/10.1016/B978-0-12-715007-9.50009-8

Potier de la Varde, R. 1943. Récoltes bryologiques de M. H. Humbert en Afrique Équatoriale. *Bull. Mus. Natl. Hist. Nat.*, ser. 2, 15: 129–133.

Proctor, M.C.F. 1977. Evidence on the carbon nutrition of moss sporophytes from $^{14}CO_2$ uptake and the subsequent movement of labelled assimilate. *J. Bryol.* 9: 375–386. http://dx.doi.org/10.1179/jbr.1977.9.3.375

Quandt, D. & Stech, M. 2005. Molecular evolution of the *trnL(UAA)* intron in bryophytes. *Molec. Phylogen. Evol.* 36: 429–443. http://dx.doi.org/10.1016/j.ympev.2005.03.014

Quandt, D., Müller, K., Stech, M., Hilu, K.W., Frey, W., Frahm, J.-P. & Borsch, T. 2004. Molecular evolution of the chloroplast *trnL-F* region in land plants. *Monogr. Syst. Bot. Missouri Bot. Gard.* 98: 13–37.

Quandt, D., Bell, N.E. & Stech, M. 2007. Unravelling the knot: The Pulchrinodaceae fam. nov. (Bryales). *Beih. Nova Hedwigia* 131: 21–39.

Rambaut, A., Suchard, M.A., Xie, D. & Drummond, A.J. 2014. Tracer, version 1.6. http://beast.bio.ed.ac.uk/Tracer

Ritzkowski, S. 1999. Das geologische Alter der Bernsteinführenden Sedimente in Sambia (Bezirk Kaliningrad), bei Bitterfeld (Sachsen-Anhalt) und bei Helmstedt (SE-Niedersachsen). Pp. 33–40 in: Kosmowska-Ceranowicz, B. & Paner, H. (eds.), *Investigations into amber: Proceedings of the international interdisciplinary symposium; Baltic amber and other fossil resins.* Gdansk: Museum of the Earth, Polish Academy of Sciences.

Ronquist, F. & Huelsenbeck, J.P. 2003. MrBayes 3: Bayesian phylogenetic inference under mixed models. *Bioinformatics* 19: 1572–1574. http://dx.doi.org/10.1093/bioinformatics/btg180

Sanderson, M.J. 2002. Estimating absolute rates of molecular evolution and divergence times, a penalized likelihood approach. *Molec. Biol. Evol.* 19: 101–109. http://dx.doi.org/10.1093/oxfordjournals.molbev.a003974

Sauquet, H., Ho, S.Y.W., Gandolfo, M.A., Jordan, G.J., Wilf, P., Cantrill, D.J., Bayly, M.J., Bronham, L., Brown, G.K., Carpenter, R.J., Lee, D.M., Murphy, D.J., Kale Sniderman, J.M. & Udovicic, F. 2012. Testing the impact of calibration on molecular divergence times using a fossil-rich group: The case of *Nothofagus* (Fagales). *Syst. Biol.* 61: 289–313. http://dx.doi.org/10.1093/sysbio/syr116

Shaw, A.J., Cox, C.J. & Goffinet, B. 2005. Global patterns of moss diversity: taxonomic and molecular inferences. *Taxon* 54: 337–352. http://dx.doi.org/10.2307/25065362

Silvestro, D. & Michalak, I. 2012. raxmlGUI: A graphical front-end for RAxML. *Organisms Diversity Evol.* 12: 335–337. http://dx.doi.org/10.1007/s13127-011-0056-0

Smith, G.L. 1971. A conspectus of the genera of Polytrichaceae. *Mem. New York Bot. Gard.* 21: 1–83.

Smith, G.L. 1974. Three new Himalayan species of *Polytrichastrum*. *J. Hattori Bot. Lab.* 38: 633–638.

Stamatakis, A. 2006. RAxML-VI-HPC: Maximum likelihood-based phylogenetic analyses with thousands of taxa and mixed models. *Bioinformatics* 22: 2688–2690. http://dx.doi.org/10.1093/bioinformatics/btl446

Swofford, D.L. 2002. PAUP*: Phylogenetic analysis using parsimony (*and other methods), version 4.0b10. Sunderland, Massachusetts: Sinauer.

Townsend, C.C. 1998. *Oligotrichum glaciale* sp. nov. and other new moss records from Kashmir. *J. Bryol.* 20: 51–64.

Wheeler, W. 2012. *Systematics: A course of lectures.* Oxford: Wiley-Blackwell. http://dx.doi.org/10.1002/9781118301081

Wiley, E.O., Siegel-Causey, D., Brooks, D.R. & Funk, V.A. 1991. *The compleat cladist: A primer of phylogenetic procedures.* Lawrence: Museum of Natural History, University of Kansas.

Yule, G.U. 1925. A mathematical theory of evolution, based on the conclusions of Dr. J. C. Willis, F.R.S. *Philos. Trans., Ser. B* 213: 21–87.

Appendix 1. Terminals sampled for molecular data including GenBank accession numbers for each marker region. For newly generated sequences (indicated by asterisks), DNA isolate number, country, region, collection number and herbarium code are provided. For previously published sequences, references to original publications precede accession numbers. A small number of previously published *nad5* sequences are concatenations of 3′ segments from one voucher and 5′ segments from another; these have the details for the 5′ segment in square brackets following the accession number for the 3′ segment.

Taxon; (DNA isolate; country, locality, collection number & herbarium code); (reference), GenBank accession numbers (18S, *rbcL, rps4-trnS, trnL-F, nad5*)

Alophosia azorica (Renauld & Cardot) Cardot; Bell & Hyvönen (2010a), GU569586, GU569408, GU569762, –, GU569491; ***Atrichum androgynum*** (Brazil); Hyvönen & al. (2004), AY126952, AY118234; Bell & Hyvönen (2010a), GU569763; Hyvönen & al. (2004), AF544999, AY137714; ***A. androgynum*** (Müll.Hal.) A.Jaeger (New Zealand); Bell & Hyvönen (2010a), GU569587, GU569409, GU569670, GU569493; ***A. angustatum*** (Brid.) Bruch & Schimp.; Bell & Hyvönen (2010a), GU569588, GU569410; Hyvönen & al. (1998), AF208417; Bell & Hyvönen (2010a), GU569671, GU569494; ***A. flavisetum*** Mitt.; Bell & Hyvönen (2010a), GU569589, GU569411, GU569765, GU569672, GU569495; ***A. oerstedianum*** (Müll.Hal.) Mitt.; Hyvönen & al. (2004), AY126953, AY118235, AY137680, AF545001, AY137716; ***A. tenellum*** (Röhl.) Bruch & Schimp.; Bell & Hyvönen (2008), EU927320, EU927308, EU927333; Bell & Hyvönen (2010a), GU569673, GU569496; ***A. undulatum*** (Hedw.) P.Beauv.; Capesius & Stech (1997), X85093; Hyvönen & al. (2004), AY118236, AY137681, AF545002; Beckert & al. (1999), AJ001229; ***Bartramiopsis lescurii*** (James) Kindb.; Hyvönen & al. (2004), AY126954; Hyvönen & al. (1998), AF208409, AF208418; Hyvönen & al. (2004), AF545003, AY137718 [+ Shaw & al. (2005), AY908800]; ***Dawsonia beccarii*** Broth. & Geh.; Bell & Hyvönen (2010a), GU569590, GU569412, GU569766, GU569674, GU569497; ***D. polytrichoides*** R.Br.; Hyvönen & al. (2004), AY126956, AY118238, AY137683, AF545005, AY137720; ***Delongia cavallii*** (G.Negri) N.E.Bell, Kariyawasam, Hedd. & Hyvönen (Uganda); Bell & Hyvönen (2008), JQ639443, JQ639452, JQ639424, JQ639414, JQ639434; ***Delongia cavallii*** (Réunion 1); N517; France, Réunion, *Hedderson 17893* (BOL); *KP901274, *KP901280, *KP901285, *KP901291, *KP901297; ***D. cavallii*** (Réunion 2); N520; France, Réunion, *Hedderson 17887* (BOL); *KP901275, *KP901281, *KP901286, *KP901292, *KP901298; ***D. cavallii*** (Tanzania); Bell & Hyvönen (2008), –, –, JQ639425, JQ639415, –; ***D. glacialis*** (C.C.Towns.) N.E.Bell, Kariyawasam, Hedd. & Hyvönen (Pakistan); Bell & Hyvönen (2008), JQ639447, JQ639456, JQ639429, JQ639419, JQ639438; ***D. glacialis*** (Sikkim); N522; India, Sikkim, *Long 22696* (E); *KP901276, *KP901287, *KP901293, *KP901299; ***D. glacialis*** (Yunnan); N524; China, Yunnan, *Long 24132* (E); *KP901277, *KP901282, *KP901288, *KP901294, *KP901300; ***Dendroligotrichum squamosum*** (Hook.f. & Wilson) Cardot; Bell & Hyvönen (2010a), GU569593, GU569415, GU569769, GU569678, GU569501; ***D. tongariroense*** (Colenso) Tangney; Bell & Hyvönen (2010a), GU569592, GU569414, GU569768, GU569677, GU569500; ***Hebantia rigida*** (Lorentz) G.L.Merr.; Bell & Hyvönen (2010a), GU569594, GU569416, GU569770, GU569679, GU569502; ***Itatiella afrolaevigata*** (Dixon) N.E.Bell & Hyvönen; Bell & Hyvönen (2010a), GU569607, GU569429, GU569783, GU569695, GU569518; ***I. ulei*** (Broth. ex Müll.Hal.) G.L.Sm.; Bell & Hyvönen (2010a), GU569595, GU569417, GU569771, GU569680, GU569503; ***Lyellia crispa*** R.Br.; Bell & Hyvönen (2008), EU927322, EU927310, EU927335; Bell & Hyvönen (2010a), GU569683, GU569506; ***Notoligotrichum bellii*** (Broth.) G.L.Sm.; Bell & Hyvönen (2010a), GU569602, GU569424, GU569778, GU569688, GU569511; ***N. tapes*** (Müll.Hal.) G.L.Sm.; Bell & Hyvönen (2010a), GU569605, GU569427, GU569781, GU569692, GU569515; ***Oligotrichum aligerum*** Mitt.; Bell & Hyvönen (2012), JQ639442, JQ639451, JQ639423, JQ639413, JQ639433; ***O. austroaligerum*** G.L.Sm.; Bell & Hyvönen (2010a), GU569608, GU569430, GU569784, GU569696, GU569519; ***O. falcatum*** Steere; Bell & Hyvönen (2012), JQ639444, JQ639453, JQ639426, JQ639416, JQ639435; ***O. falcifolium*** (Griff.) G.L.Sm.; Bell & Hyvönen (2012), JQ639445, JQ639454, JQ639427, JQ639417, JQ639436; ***O. hercynicum*** (Hedw.) Lam. & DC.; Hyvönen & al. (2004), AY126962, AY118243, AY137688, AF545014, AY137729; ***O. javanicum*** (Hampe) Dozy & Molk.; Bell & Hyvönen (2012), JQ639446, JQ639455, JQ639428, JQ639418, JQ639437; ***O. obtusatum*** Broth.; Bell & Hyvönen (2010a), GU569611, GU569433, GU569787, GU569699, GU569522; ***O. parallelum*** (Mitt.) Kindb.; Hyvönen & al. (2004), AY126963; Hyvönen & al. (1998), AF208415, AF208424; Hyvönen & al. (2004), AF545015, AY137730 [+ Shaw & al. (2005), AY908805]; ***O. suzukii*** (Broth.) C.C.Chuang; Bell & Hyvönen (2010a), GU569613, GU569435, GU569789, GU569701, GU569524; ***O. tenuirostre*** (Hook.) A.Jaeger; Bell & Hyvönen (2010a), GU569614, GU569436, GU569790, GU569702, GU569525; ***Pogonatum aloides*** (Hedw.) P.Beauv.; Bell & Hyvönen (2010a), GU569615, GU569437, GU569791, GU569703, GU569526; ***P. belangeri*** (Müll.Hal.) A.Jaeger; Bell & Hyvönen (2010a), GU569616, GU569438, GU569792, GU569704, GU569527; ***P. campylocarpum*** (Müll.Hal.) Mitt.; Bell & Hyvönen (2010a), GU569617, GU569439, GU569793, GU569705, GU569528. ***P. dentatum*** (Menzies ex Brid.) Brid.; Bell & Hyvönen (2010a), GU569621, GU569443, GU569797, GU569709, GU569532; ***P. japonicum*** Sull. & Lesq.; Bell & Hyvönen (2010a), GU569622, GU569444, GU569798, GU569710, GU569533; ***P. macrophyllum*** Dozy & Molk.; Bell & Hyvönen (2010a), GU569623, GU569445, GU569799, GU569711, GU569534; ***P. microstomum*** (R.Br. ex Schwägr.) Brid.; Bell & Hyvönen (2010a), GU569624, GU569446, GU569800, GU569712, GU569535; ***P. nipponicum*** Nog. & Osada; Bell & Hyvönen (2010a), GU569626, GU569448, GU569802, GU569714, GU569537; ***P. perichaetiale*** (Mont.) A.Jaeger; Bell & Hyvönen (2010a), GU569627, GU569449, GU569803, GU569715, GU569538; ***P. sinense*** (Broth.) Hyvönen & P.C. Wu; N455; China, Yunnan, *Long 24276* (E); *KP901278, *KP901283, *KP901289, *KP901295, *KP901301; ***P. subulatum*** (Menzies ex Brid.) Brid.; Bell & Hyvönen (2010a), GU569629, GU569451, GU569805, GU569717, GU569540; ***P. urnigerum*** (Hedw.) P.Beauv.; Hyvönen & al. (1998), AF208406; Hyvönen & al. (2004), AY118256; Hyvönen & al. (1998), AF208426; Hyvönen & al. (2004), AF545028; Beckert & al. (2001), AJ291554; ***Polytrichadelphus innovans*** (Müll.Hal.) A.Jaeger; Bell & Hyvönen (2010a), GU569636, GU569458, GU569812, GU569725, GU569548; ***P. longisetus*** (Brid.) Mitt.; Bell & Hyvönen (2010a), GU569637, GU569459, GU569813, GU569726, GU569549; ***P. purpureus*** Mitt.; Bell & Hyvönen (2010a), GU569638, GU569460, GU569814, GU569728, GU569551; ***Polytrichastrum alpinum*** (Hedw.) G.L.Sm. (New Zealand); Bell & Hyvönen (2010a), GU569640, GU569462, GU569816, GU569731, GU569554; ***P. alpinum*** (Scotland); Bell & Hyvönen (2008), EU927327, EU927315, EU927340; Bell & Hyvönen (2010a), GU569729, GU569552; ***P. altaicum*** Ignatov & G.L.Merr.; Bell & Hyvönen (2010a), GU569643, GU569465, GU569819, GU569734, GU569557; ***P. emodi*** G.L.Sm.; Bell & Hyvönen (2010a), GU569645, GU569467, GU569821, GU569736, GU569559; ***P. lyallii*** (Mitt.) G.L. Sm.; Bell & Hyvönen (2008), EU927331; Hyvönen & al. (2004), AY118241; Hyvönen & al. (1998), AF208423; Hyvönen & al. (2004), AF545011, AY137726 [+ Shaw & al. (2005), AY908802]; ***P. papillatum*** G.L.Sm.; Bell & Hyvönen (2010a), GU569652, GU569474, GU569828, GU569744, GU569567; ***P. septentrionale*** (Brid.) E.I.Ivanova, N.E.Bell & Ignatov; Bell & Hyvönen (2010a), GU569642, GU569464, GU569818, GU569733, GU569556; ***P. sexangulare*** (Canada); GU569654, GU569476, GU569830, GU569746, GU569569; ***P. sexangulare*** (Flörke ex Brid.) G.L.Sm. (Finland); Bell & Hyvönen (2010a), GU569653, GU569475, GU569829, GU569745, GU569568; ***P. sphaerothecium*** (Besch.) J.-P.Frahm (Iceland); Bell & Hyvönen (2010a), GU569657, GU569479, GU569833, GU569749, GU569572; ***P. sphaerothecium*** (Kuril Islands); Bell & Hyvönen (2010a), GU569655, GU569477, GU569831, GU569747, GU569570; ***P. tenellum*** (Müll.Hal.) G.L.Sm.; Bell & Hyvönen (2010a), GU569658, GU569480, GU569834, GU569750, GU569573; ***Polytrichum appalachianum*** L.E.Anderson; Bell & Hyvönen (2010a), GU569644, GU569466, GU569820, GU569735, GU569558; ***P. commune*** Hedw.; N376; Denmark, Faroe Islands, *Väre 17561* (H); *KP901279, *KP901284, *KP901290, *KP901296, *KP901302; ***P. ericoides*** Hampe; Bell & Hyvönen (2010a), GU569664, GU569486, GU569839, GU569755, GU569579; ***P. juniperinum*** Hedw.; Bell & Hyvönen (2008), EU927329, EU927317, EU927342; Bell & Hyvönen (2010a), GU569757, GU569581; ***P. pallidisetum*** Funck; Bell & Hyvönen (2010a), GU569651, GU569473, GU569827, GU569743, GU569566; ***P. piliferum*** Hedw.; Hyvönen & al. (2004), AY126981, AY118263, AY137706, AF545037, AY137752; ***P. torquatum*** (Mitt. ex Osada & G.L.Sm.) N.E.Bell & Hyvönen; Bell & Hyvönen (2010a), GU569659, GU569481, GU569835, GU569751, GU569574; ***Psilopilum cavifolium*** (Wilson) I.Hagen; Bell & Hyvönen (2008), EU927330, EU927318, EU927343; Bell & Hyvönen (2010a), GU569761, GU569585; ***P. laevigatum*** (Wahlenb.) Lindb.; Hyvönen & al. (2004), AY126983; Hyvönen & al. (1998), AF208416, AF208429; Hyvönen & al. (2004), AF545039, AY137754; ***Steereobryon subulirostrum*** (Schimp. ex Besch.) G.L.Sm.; Hyvönen & al. (2004), AY126984, AY118265, AY137708, AF545040, AY137755;

Appendix 2. Voucher specimens for SEM.

Taxon, country, locality, collection number, herbarium code

Delongia cavallii (specimen 1), Kenya, Mt. Kenya, *Townsend 85/290* (E); ***Delongia cavallii*** (specimen 2), Uganda, Ruwenzori Mts., *Newbould 5285* (E); ***Delongia glacialis***, India, Sikkim, *Long 22696* (E); ***Oligotrichum aligerum***, Japan, Aichi Prefecture, *Takaki s.n.*, 18.v.1952 (H); ***Oligotrichum austroaligerum***, Chile, Magallanes, *Bell 1629* (H); ***Oligotrichum obtusatum***, Nepal, Koshi, *Iwatsuki 1666* (NY); ***Oligotrichum parallelum***, U.S.A., Washington, *Schofield 47168* (H); ***Psilopilum cavifolium***, Finland, Lapland, *Bell 05.07.06.002* (H).